

February 24, 2019

Re: Resubmission of manuscript *Identifying ENSO Influences on Rainfall with Classification Models: Implications for Water Resource Management of Sri Lanka*, Ms. No. hess-2018-249

Dr. Wouter Buytaert
Editor, Hydrology and Earth System Sciences

Dear Dr. Buytaert,

Thank you for giving us the opportunity to revise our manuscript, *Identifying ENSO Influences on Rainfall with Classification Models: Implications for Water Resource Management of Sri Lanka*. We appreciate the careful review and constructive comments. We believe that the manuscript is improved after making the proposed edits to the figures.

Following this note are the editor's comments in the blue color, followed by our comments explaining how the figures were modified. Revisions were made in consultation with all the authors, and each author has approved the revised manuscript.

Thank you for your consideration.

Sincerely,



Thushara De Silva M.

Thank you for submitting your revised version of this manuscript. After careful reading of the revision, I think that the text is suitable for publication. However, the presentation, especially of the figures, suffers from some issues that can easily be addressed. In particular:

- Figure 1: the legend needs to be more precise: "Annual average precipitation [mm]". Also, the maps require a coordinate grid and scale.

The legend was revised as proposed and grid coordinates and scale were added to the map

- Figure 2: Explain in the caption the meaning of the abbreviations (NEM, FIM, SWM, SIM)

Figure 2 caption was revised as follows.

Figure 1: Sub basin Rainfall for (a) Morape, (b) Peradeniya, (c) Randenigala, (d) Bowatenna, (e) Laxapana (f) Norwood, (g) Norton Bridge, and (h) Manampitiya. Rainfall seasons are North East Monsoon (NEM), First Inter-Monsoon (FIM), South West Monsoon (SWM), and Second Inter-Monsoon (SIM)

- Figure 4: Using the "(" symbol is not ideal for readability. Can you change this for instance to a

cross or x?

Figure 4 "(" were removed, and instance with similar color code of the two other graphs (tree model) were included for the better readability.

- Figure 5: the text of this figure is very small - increase.

Figure 5 with increased font sized was included.

Once these issues are solved, I will happily accept the manuscript.

Thank you in advance for accepting the manuscript.

1 Identifying ENSO Influences on Rainfall with Classification 2 Models: Implications for Water Resource Management of Sri 3 Lanka

4 Thushara De Silva M.^{1,3}, George M. Hornberger^{1,2,3}

5 ¹Department of Civil and Environmental Engineering, Vanderbilt University, Nashville, Tennessee, USA.

6 ²Department of Earth and Environmental Science, Vanderbilt University, Nashville, Tennessee, USA.

7 ³Vanderbilt Institute for Energy and Environment, Vanderbilt University, Nashville, Tennessee, USA.

8 *Correspondence to:* Thushara De Silva M. (thushara.k.de.silva@vanderbilt.edu, thushara.k.de.silva@ieee.org)

9 **Abstract.** Seasonal to annual forecasts of precipitation patterns are very important for water infrastructure
10 management. In particular, such forecasts can be used to inform decisions about the operation of multipurpose
11 reservoir systems in the face of changing climate conditions. Success in making useful forecasts often is achieved by
12 considering climate teleconnections such as the El-Nino-Southern Oscillation (ENSO), Indian Ocean Dipole (IOD) as
13 related to sea surface temperature variations. We present a statistical analysis to explore the utility of using rainfall
14 relationships in Sri Lanka with ENSO and IOD to predict rainfall to Mahaweli and Kelani, river basins of the country.
15 Forecasting of rainfall as classes; flood, drought and normal are helpful for the water resource management decision
16 making. Results of these models give better accuracy than a prediction of absolute values. Quadratic discrimination
17 analysis (QDA) and classification tree models are used to identify the patterns of rainfall classes with respect to ENSO
18 and IOD indices. Ensemble modeling tool Random Forest is also used to predict the rainfall classes as drought and
19 not drought with higher skill. These models can be used to forecast the areal rainfall using predicted climate indices.
20 Results from these models are not very accurate; however, the patterns recognized provide useful input to water
21 resources managers as they plan for adaptation of agriculture and energy sectors in response to climate variability.

22 1 Introduction

23 The spatial and temporal uncertainty of water availability is one of the major challenges in water resource
24 management. Understanding patterns and identifying trends in seasonal to annual precipitation are very important for
25 water infrastructure management. In particular, forecasts that incorporate such information can be used to inform
26 decisions about the operation of multipurpose reservoir systems in the face of changing climate conditions.

27 Success in making useful forecasts often is achieved by considering climate teleconnections such as the El-Nino-
28 Southern Oscillation (ENSO) as related to sea surface temperature variations and air pressure over the globe using
29 empirical data (Amarasekera et.al., 1997; Denise et.al., 2017; Korecha and Sorteberg, 2013; Seibert et.al., 2017). Also,
30 modes of variability of other tropical oceans can be related to regional precipitation (Dettinger and Diaz, 2000; Eden
31 et al., 2015; Maity and Kumar, 2006; Malmgren et al., 2005; Ranatunge et al., 2003; Suppiah, 1996; Roplewski and
32 Halpert, 1996). For example, the effect of the Indian Ocean Dipole (IOD) is identified as independent of the ENSO
33 effect (Eden et al., 2015). Pacific decadal oscillation (PDO), Atlantic multi-decadal mode oscillation (AMO), ENSO,
34 and IOD teleconnections to precipitation have been found by many studies over the globe. Variations of precipitation

35 in the United States are explained by ENSO, PDO and AMO (Eden et al., 2015; National Oceanic and Atmospheric
36 Administration, 2017; Ward et al., 2014), in African countries by ENSO, AMO and IOD (Reason et al., 2006), and in
37 South east Asian countries by ENSO: Indonesia (Lee, 2015; Nur'utami and Hidayat, 2016), Thailand (Singhrattna
38 et al., 2005), China (Cao et al., 2017; Ouyang et al., 2014; Qiu et al., 2014). Australia (Bureau of Meteorology, 2012;
39 Verdon and Franks, 2005), and central and south Asia (Gerlitz et al., 2016).

40 The impact of ENSO and IOD on the position of the intertropical convergence zone (ITCZ) has been identified as a
41 primary factor driving south Asian tropical climate variations. South Asian countries get precipitation from two
42 monsoons from the movements of ITCZ in boreal summer (2°N) and boreal winter (8°S). The South western monsoon
43 (summer monsoon) is during June-August months and the North eastern monsoon (winter monsoon) is during
44 December –February months (Schneider et al., 2014). Climate teleconnections have been studied for summer
45 monsoons (Singhrattna et al., 2005; Surendran et al., 2015) and winter monsoons (Zubair and Ropelewski, 2006). A
46 negative correlation of ENSO with Indian summer monsoon has been identified (Jha et al., 2016; Surendran et al.,
47 2015).

48 The objective of this study is to explore the climate teleconnection to dual monsoons and inter monsoons. Water
49 resource management decisions typically are based on precipitation throughout the year and it is extremely important
50 to explore the possibility that rainfall might be related to teleconnection indices for which seasonal forecasts are
51 available. Sri Lanka is a South Asian country that gets rainfall from two monsoons and two inter-monsoons. We
52 explore ENSO and IOD climate teleconnection to Sri Lanka precipitation throughout the year. Past studies have
53 identified climate teleconnection linking precipitation to climate indices for several months and monsoon seasons, and
54 shown the importance of these for forecasting rainfall in river basins (Chandimala and Zubair, 2007; Chandrasekara
55 et al., 2003). We extend these analyses across monsoon and inter-monsoon seasons.

56 Although rainfall anomalies may be correlated strongly with teleconnection indices, the scatter in the data can be
57 large, making predictions from regression models have high uncertainty. However, water managers may act on
58 information about whether rainfall is expected to be abnormally low or high. Seasonal precipitation is generally
59 forecasted in broad categories. For example, the US National Weather Service forecasts seasonal precipitation as
60 above normal, below normal, and normal (National Oceanic and Atmospheric Administration, 2018). The
61 International Research Institute for Climate and Society also forecasts seasonal precipitation as above, below and near
62 normal (International Research Institute for Climate Society, 2018). We chose to follow a similar approach and
63 investigate river basin rainfall teleconnections to climate indices with classification models. If reasonably accurate
64 relationships can be developed, they will be useful for water resources management. For example, in Sri Lanka
65 decisions about allocations of water for irrigation and hydropower could be improved with estimates of when low
66 rainfall seasons are likely.

67 **2 Hydrometeorology and climatology of the study area**

68 Sri Lanka is an island in the Indian Ocean (latitude $5^{\circ}55' \text{N}$ - $9^{\circ}50' \text{N}$, longitudes $79^{\circ}40' \text{E}$ – $81^{\circ}53' \text{E}$). Mean annual
69 rainfall varies from 880 mm to 5500 mm across the island. The rainfall distribution is determined by the monsoon
70 system of the Indian Ocean interacting with the elevated land mass in the interior of the country. The country is divided

71 into three climatic zones according to the rainfall distribution: humid zone (wet zone) (annual rainfall > 2500 mm),
72 intermediate zone (2500 mm < rainfall < 1750 mm) and arid zone (dry zone) (rainfall < 1750 mm) (Department of
73 Agriculture Sri Lanka, 2017).

74 Sri Lanka, a water-rich country, has 103 river basins varying from 9 km² to 10448 km². A large fraction of the water
75 resources management infrastructure of the country is associated with the Mahaweli and Kelani river basins. The
76 catchment areas of the Mahaweli and Kelani are 10448 km² and 2292 km² respectively. The two rivers start from the
77 central highlands. Mahaweli, the longest river, travels to the ocean 331 km in the eastern direction and the Kelani 145
78 km in the western direction. Average annual discharge volume for the Mahaweli and Kelani basins are 26368 10⁶m³
79 and 8660 10⁶m³ respectively (Manchanayake and Madduma Bandara, 1999). The Kelani river basin is totally inside
80 the humid zone whereas the Mahaweli river basin migrates through all three climate zones (Fig.1).

81 The temporal pattern of rainfall in Sri Lanka can be divided into four seasons as follows.

82 (1) Generally low precipitation across the country from the Northeast monsoon (NEM), which gets most precipitation
83 during January to February. The arid zone of the country gets significant precipitation from the NEM, while
84 humid zone gets very little rainfall during this period.

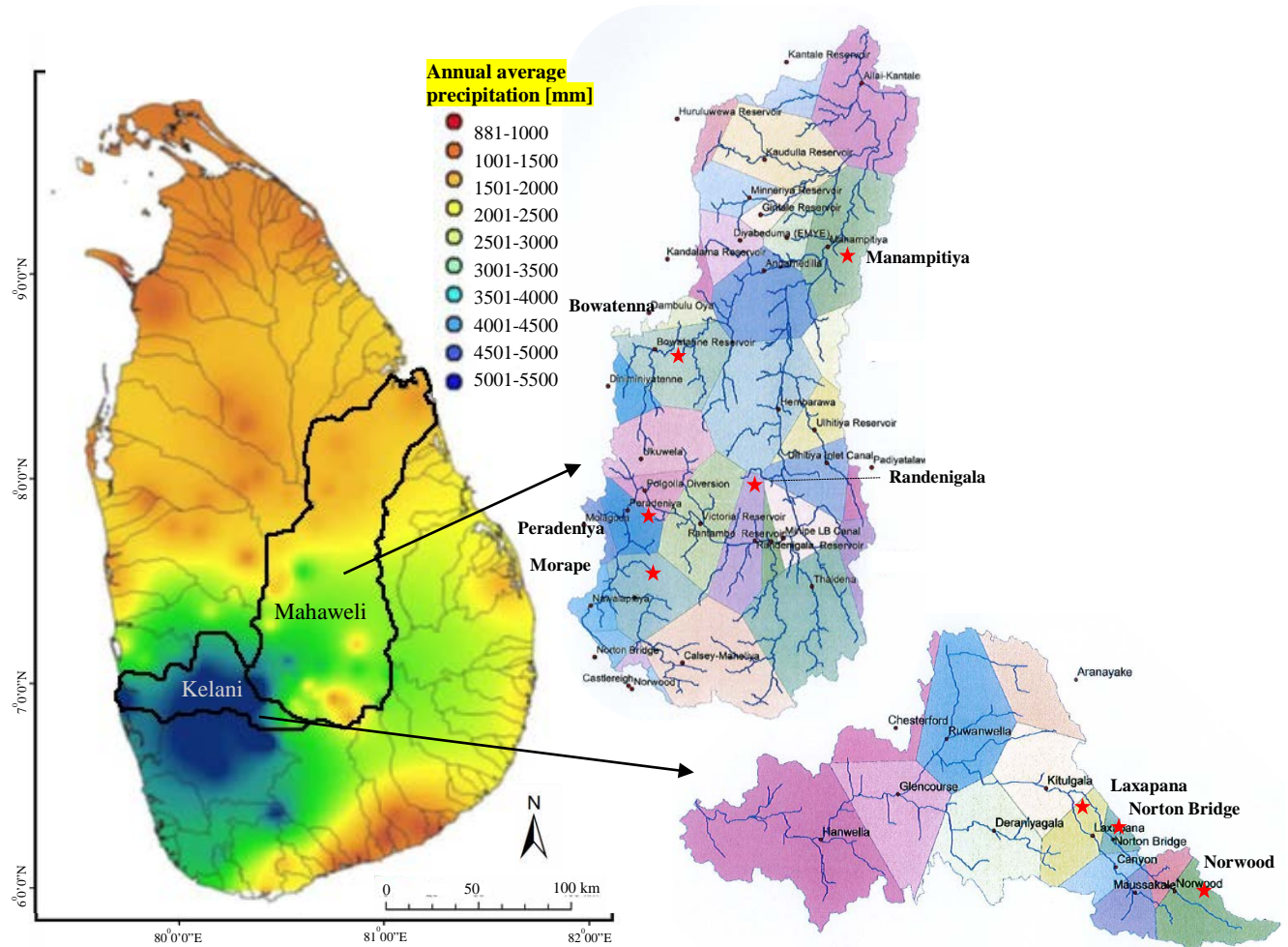
85 (2) The whole country gets precipitation from the first inter-monsoon (FIM) during March to April months. However,
86 rainfall during this period is not very high across the country.

87 (3) The highest precipitation for the country is from the South western monsoon (SWM) during May to September.
88 However, only the humid zone gets high precipitation during this season.

89 (4) The whole country gets precipitation from the second inter-monsoon (SIM) during October to December.
90 Generally, precipitation from SIM is higher than FIM.

91 The time period of NEM and SIM are generally considered as December to February and October to November
92 respectively (Department of Meteorology Sri Lanka, 2017; Malmgren et.al, 2003; Ranatunge et al., 2003). However,
93 considering the bulk amount of water received from the monsoon, we consider January and February as the period of
94 NEM and October to December as the period of SIM.

95 Reflecting the rainfall seasons, the country has two agriculture seasons “Yala” (April - September) and “Maha”
96 (October - March). Because the arid zone gets minimal precipitation during the SWM, the agricultural systems
97 (165,000 ha) developed under the Mahaweli multipurpose project depend on irrigation water during the Yala season.
98 The country depends on stored water to drive hydropower year round. The Mahaweli and Kelani hydropower plants
99 of 810 MW and 335 MW capacity serve as peaking and contingency reserve power to the power system (Ceylon
100 Electricity Board, 2015). Management of reservoir systems is done to cater both to irrigation and hydropower
101 requirements.



102

103

Figure 1 Mahaweli and Kelani river basins of Sri Lanka

104 **2.1 Sub-basin rainfall (Areal rainfall)**

105

106 Monthly rainfall data for years 1950-2013 are used for the study (Ceylon Electricity Board, 2017). River basin rainfall
 107 was calculated using the Thiessen polygon method (Viessman, 2002). The Mahaweli river basin is divided into 16
 108 Thiessen polygons and the Kelani river basin is divided into 11 Thiessen polygons (Figure 1). Since this study does
 109 not aim to explore rainfall across sub-basins, we do not use digital elevation maps to define the sub-basins. Considering
 110 the importance of sub-basins for the reservoir catchment and for water use, eight sub-basins are selected for analysis.
 111 Morape, Randenigala, Peradeniya, Manampitiya and Bowatenna represent the Mahaweli major reservoir catchments
 112 and irrigation tanks, and Norton Bridge, Norwood and Laxapana represent the Kelani basin reservoir catchments. The
 113 catchment of the major Mahaweli river reservoir cascade (Kotmale, Victoria, Randenigala, Rantambe, Bowatenna) is
 114 represented by Morape and Peradeniya located in the humid zone and by Randenigala and Bowatenna located in the
 115 intermediate zone. The arid zone major irrigation catchments of the Mahaweli are represented by Manampitiya. The
 116 catchment of the Kelaniya reservoir cascade (Norton Bridge and Moussakele) in the humid zone is represented by
 117 Laxapana, Norton Bridge and Norwood.

118 We calculate the rainfall for the four seasons, NEM, FIM, SWM and SIM for 64 years of historical data. Rainfall
 119 anomalies are calculated by reducing the seasonal mean rainfall (Eq.(1)) and standardized anomalies are calculated
 120 by dividing the rainfall anomalies by the standard deviation (SD) (Eq.(2)).

$$X_{ANM} = (X - \bar{X}_t) \quad \text{Eq.(1)}$$

$$X_{S_ANM} = (X - \bar{X}_t)/SD_t \quad \text{Eq.(2)}$$

121 Where, \bar{X}_t is the average of seasonal rainfall, X_{ANM} is the rainfall anomaly and X_{S_ANM} is the standardized rainfall
 122 anomaly.

123 Standardized rainfall anomalies are divided into three classes as dry, average and wet (Table 1). A normality test for
 124 the rainfall data classes is done using the Shapiro-Wilk test. If the rainfall data are not normally distributed, log (e),
 125 square root or square functions are used to transform the data into normally distributed data sets (Fig. A 1). Extreme
 126 seasonal precipitation has been defined statistically in different ways using statistical thresholds (Easterling et al.,
 127 2000; Jentsch et.al., 2015; Smith, 2011). We use 0.5 as a threshold to define three classes, which results in fairly
 128 evenly distributed data across the three classes (Fig. A 2).

129 **Table 1** Rainfall anomaly classification

Class	Range
dry	$X_{S_ANM} < -0.5$
average	$-0.5 \leq X_{S_ANM} < 0.5$
wet	$0.5 \leq X_{S_ANM}$

130 **2.2 ENSO & IOD indices**

131 The ENSO phenomenon is represented by MEI, NINO34, NINO3, NINO4 indices, and the Indian Ocean dipole
 132 phenomenon is represented by DMI index. NINO34, NINO3, NINO4 indices are based on tropical sea surface
 133 temperature anomalies (National Center for Atmospheric Research, 2018) and the Multivariate ENSO Index (MEI) is
 134 based on sea-level pressure, zonal and meridional components of the surface wind, sea surface temperature, surface
 135 air temperature, and total cloudiness fraction of the sky (National Oceanic and Atmospheric Administration, 2017).
 136 The Indian Ocean Dipole (IOD) is an oscillation of sea surface temperature in the equatorial Indian ocean between
 137 Arabian sea and south of Indonesia (Bureau of Meteorology Australia, 2017). IOD is identified as relevant to the
 138 climate of Australia (Power et.al., 1999) and countries surrounded by the Indian ocean in southern Asia (Chaudhari et
 139 al., 2013; Maity and Nagesh Kumar, 2006; Qiu et al., 2014; Surendran et al., 2015). The Dipole Mode Index (DMI)
 140 is used to represent the IOD capturing the west and eastern equatorial sea surface temperature gradient.

141 Data used for the analyses are NINO34, NINO3, NINO4, MEI monthly data from years 1950 – 2013, (National
 142 Oceanic and Atmospheric Administration, 2017; National Center for Atmospheric Research, 2018), and the DMI
 143 monthly data from years 1950-2013 (HadISST dataset, Japan Agency for Marine-Earth Science and Technology
 144 2017). Because we analyzed the data in rainfall seasons, values of the climate indices over the season are averaged.
 145 For example for the NEM season, the MEI value is the average of January and February monthly values and for the
 146 SWM season, DMI is the average of May, June, July and September values.

147 **3 Methods**

148 Seasonal values of MEI and DMI were used as the predictors to classify seasons into the three rainfall classes. The
 149 total data set is divided into 75 % for training the model and 25 % for testing model performance. Quadratic
 150 discriminant analysis (QDA) and classification trees were selected for the analyses. A random forest model also was
 151 applied to investigate the reliability of a cross-validated statistical forecast tool based on an advance estimate of MEI
 152 and DMI. We used the R programming language to carry out the statistical analyses. R packages: caret, tree,
 153 randomForest, fitdistrib, devtools and quantreg are used for the studies.

154 **3.1 Quadratic Discriminant Analysis (QDA)**

155 The mathematical formulation of QDA can be derived from Bayes theorem assuming that observations from each
 156 class are drawn from a Gaussian distribution (James et.al., 2013; Löwe et.al., 2016).

157 The prior probability π_k represents the randomly chosen observation coming from kth class with density
 158 function $f_k(x)$. Bayes theorem states that

$$Pr(Y = k|X = x) = \frac{\pi_k f_k(x)}{\sum_{l=1}^K \pi_l f_l(x)} \quad \text{Eq.(3)}$$

159 In Eq.(3), the posterior probability $Pr(Y = k|X = x)$ indicates that observation $X = x$ belongs to the kth class. For p
 160 predictors, the multivariate Gaussian distribution density function is defined for every class k (Eq.(4)).

$$f_k(x) = \frac{1}{(2\pi)^{p/2} |\Sigma_k|^{1/2}} \exp\left(-\frac{1}{2}(x - \mu_k)^T \Sigma_k^{-1} (x - \mu_k)\right) \quad \text{Eq.(4)}$$

161 In Eq.(2), Σ_k is the covariance matrix and μ_x is the mean vector. The covariance matrix (Σ_k) and mean (μ_x) for each
 162 class are estimated from the training data set (Eq.(5), Eq.(6)).

$$\mu_k = \frac{1}{N_k} \sum_{i:y_i=k} x_i \quad \text{Eq.(5)}$$

$$\Sigma_k = \frac{1}{(N_k - 1)} \sum_{i:y_i=k} (x_i - \mu_k)^T (x_i - \mu_k) \quad \text{Eq.(6)}$$

163 Substituting a Gaussian density function for the kth class (Eq.(4)) into Bayes theorem and taking the log values, the
 164 quadratic discriminant function is derived (Eq.(7)). Prior probabilities for class k (π_k) is calculated by the frequency
 165 of data points of class k in the training data (Eq.(8)). For a total number of N points in the training observations, N_k is
 166 the number of observations belong to kth class.

$$\delta_k(x) = -\frac{1}{2} (x - \mu_k)^T \Sigma_k^{-1} (x - \mu_k) + \log \pi_k \quad \text{Eq.(7)}$$

$$\pi_k = \frac{N_k}{N} \quad \text{Eq.(8)}$$

167 Covariance, mean and prior probability values are inserted into the discriminant function ($\delta_k(x)$) together with the
 168 state variables (Eq.(5)). The corresponding class is selected according to the largest value of the function. The number
 169 of parameters to be estimated for the QDA model for k classes and p predictors is $k \cdot p \cdot (p + 1) / 2$. For this study, the
 170 QDA model output is the probability that an observation of a climate category will fall into each of the rainfall classes.

171 **3.2 Classification Tree model**

172 For the classification tree model the predictor space is divided into non-overlapping regions ($R_1..R_j$). A classification
173 tree predicts each observation as belonging to the most commonly occurring class of the training data regions (James
174 et.al., 2013). Recursive binary splitting is used to grow the classification tree.

175 Classification error rate, Gini index and cross-entropy are typically used to evaluate the quality of particular split
176 (James et.al., 2013), and in our study we used the first two indices. Classification error rate (E) gives fraction of
177 observation that do not belong to the most commonly occurring class of the training data regions (Eq.(9)). However,
178 for the tree-growing, the Gini index (G) is considered as the criterion for splitting into regions (Eq.(10))

$$E = 1 - \max_k(\hat{p}_{mk}) \quad \text{Eq.(9)}$$

$$G = \sum_{k=1}^K \hat{p}_{mk} (1 - \hat{p}_{mk}) \quad \text{Eq.(10)}$$

179 In Eq.(9) and Eq.(10), \hat{p}_{mk} represents the fraction of observations in the m^{th} class that belong to the k^{th} class. The Gini
180 index is considered as a measure of node purity of the tree model, since small values of the index indicate that node
181 has a higher number of observations from a single class.

182 The complexity of the trees are adjusted using a pruning process to produce more interpretable results. Complex trees
183 reduces training error by overfitting the training data. Simple trees can be interpreted well, however, selecting a model
184 which can find the pattern of data is important. In order to achieve the low classification error (training error + testing
185 error), pruning technique is used. First, grow the very large tree, and sub tree is obtained by removing the weak links
186 of the tree. Using tuning parameter to examine the trade-off between complexity of tree and the training error, and
187 defining minimum samples for a node, maximum depth of the tree, and maximum number of terminal nodes are some
188 of the pruning methods (Analytical Vidhya Team, 2016). For this study, we defined the maximum number of nodes
189 to obtain the simple tree (pruned tree).

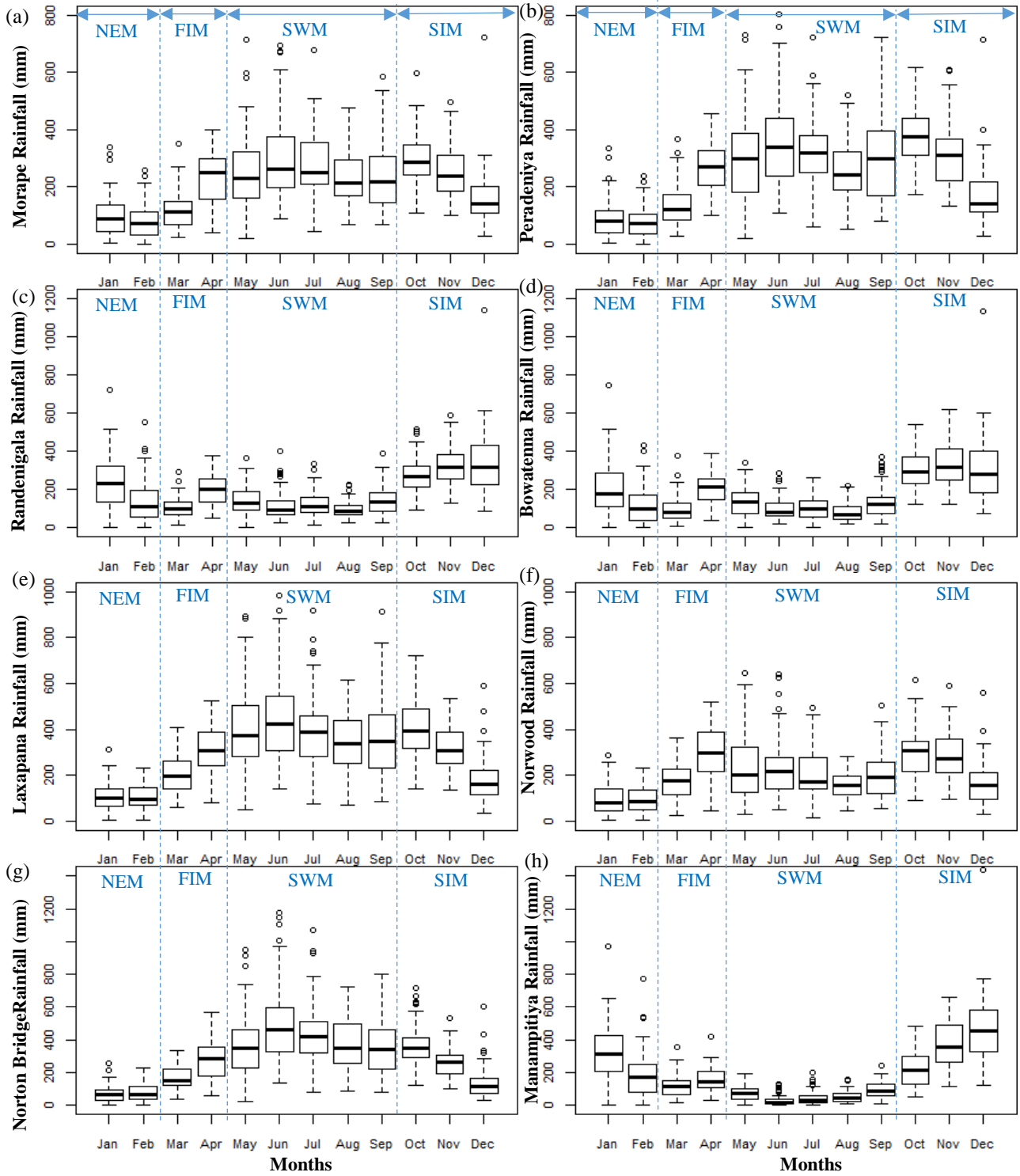
190 Tree models give the probability that an observation falls into each of the three rainfall classes. The predicted class is
191 assigned based on the highest probability. Tree models handle ties of probability values by randomly assigning the
192 class.

193 **3.3 Random Forest**

194 A random forest is an ensemble learning method used for classification and regression problems. The method is based
195 on a multitude of decision trees based on training data with the final model as the mean of the ensemble (Breiman,
196 2001). Individual trees are built on a random sample of the training data with several predictors from the total number
197 of predictors. Individual trees are built from the bootstrapped training data set.

198 There are some features, which can be tuned to make the better performed random forest model. Maximum number
199 of predictors from the total predictors for individual trees, maximum number of trees, maximum node size of the trees
200 and minimum sample leaf size are some of these features (Analytical Vidhya Team, 2015). In our study, we use the
201 maximum number of trees as the main tuning parameters.

202 In a random forest model the importance of the variable is measured as the decrease in node impurity from the splits
203 over the variable. This value is calculated by averaging the Gini index over the multitude of trees with a larger value
204 indicating high importance of the predictor (James et.al., 2013).



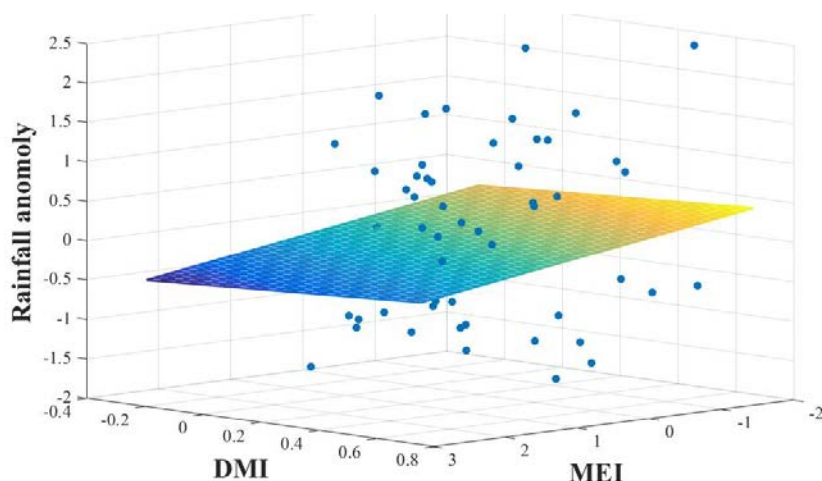
205

206 **Figure 2:** Sub basin Rainfall for (a) Morape, (b) Peradeniya, (c) Randenigala, (d) Bowatenna, (e) Laxapana (f)
 207 Norwood, (g) Norton Bridge, and (h) Manampitiya. Rainfall seasons are North East Monsoon (NEM), First Inter-
 208 Monsoon (FIM), South West Monsoon (SWM), and Second Inter-Monsoon (SIM)

209 **4 Results**

210 Monthly rainfall boxplots of eight sub basins over the year for 1950 - 2013 illustrate the seasonal and the spatial
211 variation of rainfall patterns (Fig. 2). The largest fraction of total rainfall in the arid zone occurs at the end of the SIM
212 (December) and during the NEM (January - February) with correspondingly high variability whereas there is little
213 rainfall in the arid zone during the SWM (May - September) with correspondingly little variability (Fig. 2 (h)). The
214 intermediate zone receives approximately 60% of total rainfall from the SIM and NEM. Although the variability of
215 the rainfall is low in the intermediate zone, high rainfall can occur in all seasons (Fig. 2 (c) and (d)). In the humid
216 zone, a large portion of rainfall occurs in SWM and early months of SIM (October-November). High variability of
217 humid zone rainfall is observed at the end of FIM (April), in the SWM (May-September), and at the start of SIM
218 (October) (Fig. 2 (a), (b), (e), (f) and (g)).

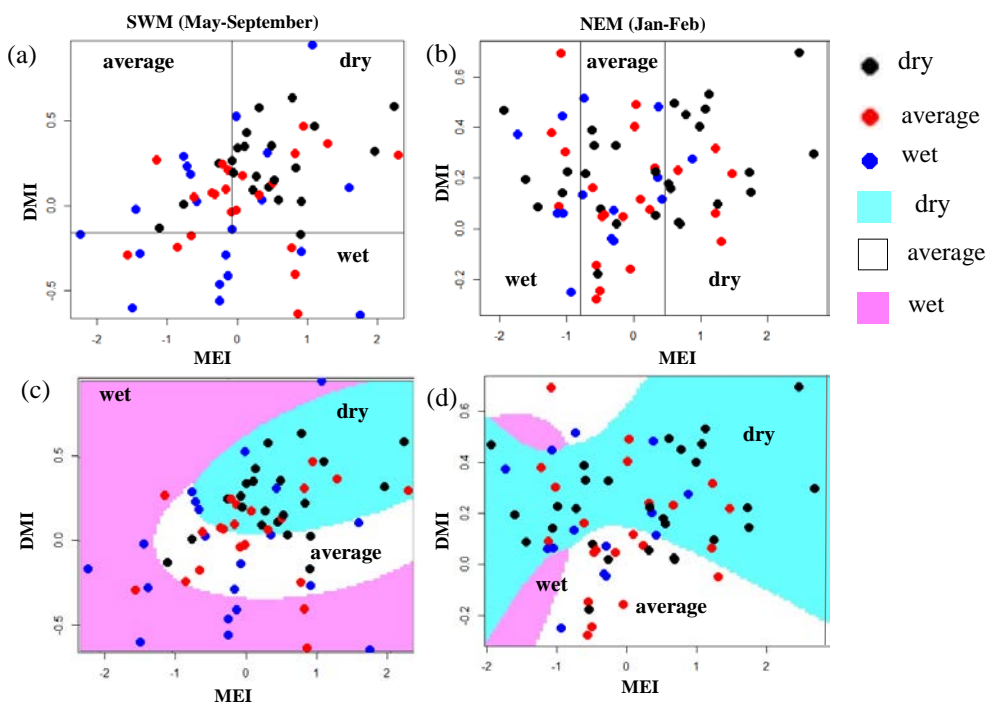
219 Similar to other investigators, we observe several strong correlations between rainfall anomalies and the climate
220 indices (Table A. 1, Table A. 2, and Appendix). Higher correlation values between MEI and rainfall anomalies can
221 be seen compared to the correlation with other ENSO indices (Table A. 1). In addition, rainfall in the SWM is very
222 important for stations in the humid zone of the country which is the source of a large amount of water stored in
223 reservoirs (Table A. 2). Correlation coefficients between SWM rainfall at Norton Bridge are negative and strong, -
224 0.31 for MEI ($p = 0.01$) and -0.37 for DMI ($p < 0.01$). The strength of the correlation notwithstanding, the residuals
225 from a regression model indicate that high uncertainty would attach to any forecast (Fig. 3). Thus, we are led to
226 explore the efficacy of classification methods (Appendix).



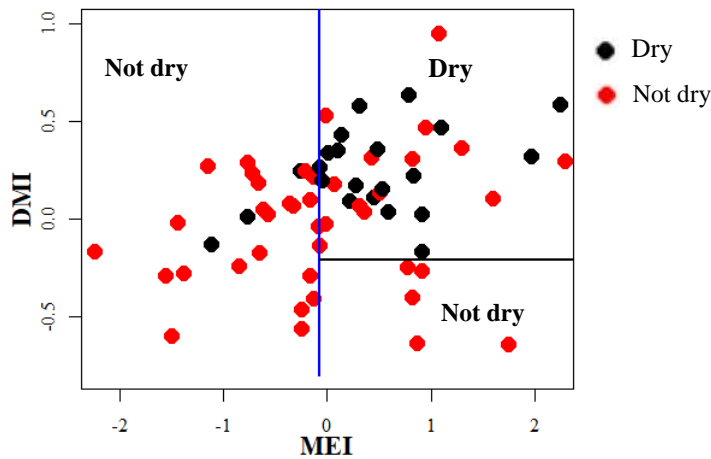
227
228 **Figure 3** Linear regression of rainfall anomaly on MEI and DMI. High values of MEI and DMI are associated with
229 low values of rainfall.

230 We present classification results for two sub-basins, one that has the highest rainfall during the NEM, Manampitiya,
231 and one that has the highest rainfall for the SWM, Norton Bridge (Fig. 4). Norton Bridge represents the areal rainfall
232 of reservoir catchments in the wet zone and Manampitiya represents the rainfall that contributes to irrigation tanks in
233 the dry zone. Results of other sub-basins are presented in the supplementary materials (Fig. A 4, Fig. A 5, Fig. A 6,
234 Fig. A 7, Appendix). Because MEI has higher correlation with rainfall anomalies than other ENSO indices,
235 classification was done with only MEI and DMI.

236 The SWM is a season when the humid zone receives the bulk of rainfall. At Norton Bridge, the occurrences of the dry
 237 rainfall anomaly class in the SWM is seen to “clump” in the region of relatively high MEI and DMI. Both the
 238 classification tree and the QDA successfully identify the pattern (Fig. 4 (a) and (c)) with an overall accuracy of 73 %,
 239 19 and 16 correct out of 22 occurrences (Table 2). In the arid zone the NEM season is one of the most important for
 240 rainfall. At Manampitiya, the MEI provides the primary variable in the classification, with the dry anomaly class being
 241 correctly selected in 52 % by tree model and 95 % with the QDA model. The results suggest that it may be possible
 242 to identify seasons when it is expected to be anomalously dry. The correct classification of “average” conditions likely
 243 has less importance for water managers. We explored classification using two classes, “Dry” and “Not Dry.” In this
 244 case, the classification model again correctly classifies 86 % of the anonymously dry cases and gets more than 69 %
 245 of the “Not Dry” cases correct (Fig. 5).



246
 247 **Figure 4** Norton Bridge and Manampitiya rainfall classes (dry, average, wet) identified by ENSO and IOD
 248 phenomena. (a) Norton Bridge SWM rainfall classification tree model (b) Manampitiya NEM rainfall classification
 249 tree model (c) Norton Bridge SWM rainfall QDA (d) Manampitiya NEM rainfall classification by QDA



250

251 **Figure 5** Classification tree for Norton Bridge SWM rainfall using two categories (dry and not dry)

252 **Table 2** Classification model results. Highlighted cells indicate where there may be information content with respect
 253 to forecasting either dry or wet anomaly classes as judged by a classification success rate of at least 2/3.

Season	Manampitiya			Norton Bridge		
	QDA Model			QDA Model		
	Dry	Normal	Wet	Dry	Normal	Wet
NEM	22/23	11/25	1/16	5/20	25/29	2/15
FIM	9/21	20/24	5/19	3/20	14/23	14/20
SWM	2/21	30/27	2/16	16/22	9/22	9/20
SIM	17/25	13/20	7/19	7/22	15/22	11/20
Season	Tree Model			Tree Model		
	Dry	Normal	Wet	Dry	Normal	Wet
	NEM	12/23	9/25	11/16	11/20	18/29
FIM	9/21	19/24	8/19	13/21	6/23	15/20
SWM	6/21	25/27	7/16	19/22	8/22	9/20
SIM	20/25	0/20	17/19	19/22	5/22	14/20

254

255 Classification trees are known to be unstable. That is, small changes in the observations can lead to large changes in
 256 the decision tree. The random forest approach overcomes the issue by building a “bag” of trees from bootstrap samples.
 257 The robustness of the model can then be checked by considering the “out-of-bag” error. The results of the random
 258 forest indicate that predictions of three rainfall anomaly classes using MEI and DMI is not feasible (Table 3). The out-
 259 of-bag error rate is close to two thirds, which for three categories is equivalent to a random selection.

260

261 **Table 3** Results of random forest ensemble classification results

Season	Norton Bridge				Manampitiya			
	Dry	Normal	Wet	OOB Er	Dry	Normal	Wet	OOB Er
NEM	11/20	12/29	6/15	55%	14/23	10/25	5/16	55%

FIM	7/21	8/23	8/20	64%	10/21	11/24	6/19	58%
SWM	9/22	6/22	8/20	64%	6/21	17/27	5/16	56%
SIM	13/22	9/22	9/20	52%	15/25	8/20	7/19	53%

262

263 However, the results of the random forest for a classification as either “Dry” or “Not Dry” suggests that there may
 264 be skill in such a prediction. The out-of-bag error rates for this case range from 22 % to 38 % for Norton Bridge and
 265 Manampitiya (Table 3) and from 20 % to 39 % across all stations (Table A. 7).

266 **Table 4** Results of random forest ensemble classification results for two rainfall anomaly classes

Season	Norton Bridge			Manampitiya		
	Dry	Not dry	OOB Error	Dry	Not dry	OOB Error
NEM	9/20	36/44	30 %	13/23	33/41	28 %
FIM	5/21	35/43	38 %	8/21	35/43	33 %
SWM	9/22	32/42	36 %	5/16	34/43	39 %
SIM	10/22	36/42	28 %	16/25	34/39	22 %

267

268 The QDA method produces results that are promising with respect to identification of extreme dry events as
 269 indicated by seasonal rainfall (Table 5).

270 **Table 5** Classification results for extreme dry (very low rainfall) and wet (very high rainfall) seasons.

Class	Range	NortonBridge SWM		Manampitiya NEM	
		tree	QDA	tree	QDA
Very dry	$X_{S_ANM} < -1.0$	10/11	10/11	6/11	11/11
dry	$-1.0 \leq X_{S_ANM} < -0.5$	9/11	6/11	5/11	9/10
average	$-0.5 \leq X_{S_ANM} < 0.5$	8/22	9/22	9/25	11/25
wet	$0.5 \leq X_{S_ANM} \leq 1.0$	5/11	5/11	1/5	0/5
Very wet	$1.0 \leq X_{S_ANM}$	6/11	6/11	7/11	1/11

271

272 5 Discussion

273 Understanding seasonal rainfall variability across the spatially diverse Mahaweli and Kelani river basins is important
 274 for irrigation and hydropower water planning. SWM and SIM are the key rainfall seasons for sub basins in the humid
 275 zone (Norton Bridge, Morape, Peradeniya and Laxapana), delivering 80 % of annual rainfall (Fig. 2 (a),(b),(e),(f)).
 276 For the arid zone (Manampitiya) and intermediate zone (Randenigala, Bowatenna) sub basins, the major season is
 277 SIM, which delivers more than 40 % of annual rainfall (Fig. 2 (c),(d),(h)). The arid zone also gets rainfall during the
 278 NEM (24 % of annual rainfall at Manampitiya) and the intermediate zone gets rainfall during the SWM (25 % - 30 %
 279 of annual rainfall at Randenigala and Bowatenna).

280 Climate teleconnection indices are related to rainfall anomalies observed during the two main growing seasons, Yala
281 and Maha. The Maha agriculture season (October-March) depends on rain from SIM and NEM. During El Nino events
282 rainfall increases for the first three months of the Maha season (SIM: October-December) (Fig. A 4, Fig. A 5, Fig. A
283 6, Fig. A 8) (Ropelewski and Halpert, 1995) and decreases during the last three months (NEM: January-March)(Fig.
284 4 (b)). In Yala season (April-September), La-Nina events enhance the rainfall during SWM (Fig. 4(a), (c), Fig. A 4,
285 Fig. A 5, Fig. A 6, Fig. A 8)(Whitaker et.al, 2001). During El Nino events the SWM rainfall is reduced (Fig. 4 (a), (c),
286 Fig. A 8, Fig. A 9) (Chandrasekara et.al, 2017; Chandimala and Zubair, 2007; Zubair, 2003). The El Nino impact
287 during the SWM is not as significant as it is during the NEM season (International Research Institute, 2017a). We
288 find, however, that there is an interaction between two teleconnection indices, MEI and IOD for SWM rainfall. During
289 the Yala season there is a high probability of having a drought when both the IOD and MEI are positive (Fig. 5). Also
290 not having drought is probable when both the IOD and MEI are negative (Fig. 5, Fig. A 8, Fig. A 9).

291 Classification of wet, average, and dry rainfall anomalies using the MEI and DMI indices is successful. For example,
292 a dry SWM season for Norton Bridge (Table 2) and other humid-zone stations (Table A. 4) is classified correctly with
293 greater than 70 % accuracy with QDA and tree models. However, a random forest approach demonstrates that there
294 is little skill in identifying a full wet-average-dry classification. However, a random forest model using only two
295 rainfall categories shows more than 60 % accuracy in identifying “dry” and “not dry” classes of key rainfall seasons
296 of the humid zone (Table 4, Table A. 7). Similarly, for arid zone locations such as Manampitiya, the dry rainfall class
297 identification for NEM and SIM seasons is about 60 % (Table 4, Table A. 7).

298 Our statistical classification models can be combined with MEI and DMI forecasts to indicate the season-ahead
299 expectation for rainfall. ENSO forecasts are available from the International Research Institute for Climate and Society
300 (International Research Institute, 2017b) and IOD forecasts are available in the Bureau of Meteorology (BOM),
301 Australian Government (Bureau of Meteorology, 2017). ENSO and IOD predictions are also associated with the
302 uncertainty. Therefore, final forecast accuracy is a combination of the MEI, DMI forecast uncertainties and model’s
303 accuracy rate in each class. Although overall prediction accuracy is not extremely high, a forecast of an anomalously
304 low rainfall season can have value for risk-averse farmers (Cabrera et.al., 2007) and can guide plans for hydropower
305 management (Block and Goddard, 2012).

306 The electricity and agriculture sectors of Sri Lanka heavily rely on Mahaweli and Kelani river water resources so
307 season ahead forecasts of abnormally low rainfall should be useful for decisions on adaptation measures. For example,
308 water availability of the first three months of a growing season is important for crop selection and the extent of land
309 to be cultivated. Hydropower planning and scheduling of maintenance of the power plants also can benefit from
310 season-ahead forecasts. The damage that can occur due to incorrect rainfall forecasts in the agriculture and energy
311 sectors can be minimized with emergency planning during the season, which is the usual practice.

312 Although the accuracy of predicting low or not low seasonal rainfall is not very high, decisions based on forecasts that
313 are improvements over climate averages should be an improvement over current practices. The accuracy of statistical
314 models can be improved with longer records, which are important to train the classification models. Also, models can
315 be fine-tuned for important shorter periods such as crop planting months and harvesting months for irrigation water
316 planning.

317 **6 Conclusion**

318 ENSO and IOD phenomena teleconnections with river basin rainfall provide potentially useful information for water
319 resource management. Relationships identified between teleconnection indices and river basin rainfall agree with other
320 research findings. Prediction of seasonal rainfall classes from ENSO and IOD indices can inform water resources
321 managers in reservoir operation planning for both hydropower and irrigation releases.

322 **Author contributions.**

323 TDM and GMH conceptualized the study and TDM carried out the data analysis. TDM prepared the paper with
324 contribution from GMH.

325 **Acknowledgement.**

326 This research is part of a multidisciplinary research initiative called Agricultural Decision-Making and Adaptation to
327 Precipitation Trends in Sri Lanka (ADAPT-SL) at Vanderbilt Institute for Energy and Environment (VIEE). The work
328 is supported by WSC Program Grant No. NSF-EAR 1204685.

329

330 **References:**

331 Amarasekera, K. N., Lee, R. F., Williams, E. R., & Eltahir, E. A. B.: ENSO and the natural variability in the flow
332 tropical rivers. *Journal of Hydrology*, 200(1–4), 24–39, [https://doi.org/10.1016/S0022-1694\(96\)03340-9](https://doi.org/10.1016/S0022-1694(96)03340-9), 1997

333 Analytical Vidhya Team. (2015). Tuning the parameters of your Random Forest model., available at:
334 <https://www.analyticsvidhya.com/blog/2015/06/tuning-random-forest-model/>, last access: 12 March 2018

335 Analytical Vidhya Team. (2016). A Complete Tutorial on Tree Based Modeling from Scratch., available at:
336 <https://www.analyticsvidhya.com/blog/2016/04/complete-tutorial-tree-based-modeling-scratch-in-python/>, last
337 access: 12 March 2018

338 Block, P., & Goddard, L.: Statistical and Dynamical Climate Predictions to Guide Water Resources in Ethiopia,
339 138(June), 287–298. [https://doi.org/10.1061/\(ASCE\)WR.1943-5452.0000181](https://doi.org/10.1061/(ASCE)WR.1943-5452.0000181), 2012.

340 Breiman, L.: Randomforest2001. *Machine Learning*, 45(1), 5–32. <https://doi.org/10.1017/CBO9781107415324.004>,
341 2001.

342 Bureau of Meteorology.: Record-breaking La Niña events. Bureau of Meteorology, 26. Retrieved from
343 <http://www.bom.gov.au/climate/enso/history/La-Nina-2010-12.pdf>, 2012.

344 Bureau of Meteorology.: Indian Ocean, POAMA monthly mean IOD forecast., available at:
345 <http://www.bom.gov.au/climate/enso/#tabs=Indian-Ocean>, 2017, last access: 30 March 2017

346 Cabrera, V. E., Letson, D., & Podesta, G.: The value of climate information when farm programs matter, 93, 25–42.
347 <https://doi.org/10.1016/j.agsy.2006.04.005>, 2007.

348 Cao, Q., Hao, Z., Yuan, F., Su, Z., Berndtsson, R., Hao, J., & Nyima, T.: Impact of ENSO regimes on developing-
349 and decaying-phase precipitation during rainy season in China. *Hydrology and Earth System Sciences*, 21(11),
350 5415–5426, 2017.

351 Ceylon Electricity Board.: Long Term Generation Expansion Plan 2015-2034. available at:
352 <http://pucsl.gov.lk/english/wp-content/uploads/2015/09/Long-Term-Generation-Plan-2015-2034-PUCSL.pdf>, 2015,

- 353 last access: 1 September 2017.
- 354 Ceylon Electricity Board.: River Basin Hydrology Data, System control branch Transmission Division. Sri Lanka,
355 2017.
- 356 Chandimala, J., & Zubair, L.: Predictability of stream flow and rainfall based on ENSO for water resources
357 management in Sri Lanka. *Journal of Hydrology*, 335(3–4), 303–312, <https://doi.org/10.1016/j.jhydrol.2006.11.024>,
358 2007.
- 359 Chandrasekara, S., Prasanna, V., & Kwon, H. H.: Monitoring Water Resources over the Kotmale Reservoir in Sri
360 Lanka Using ENSO Phases. *Advances in Meteorology*, <https://doi.org/10.1155/2017/4025964>, 2017.
- 361 Chaudhari, H. S., Pokhrel, S., Mohanty, S., & Saha, S. K.: Seasonal prediction of Indian summer monsoon in NCEP
362 coupled and uncoupled model. *Theoretical and Applied Climatology*, 114(3–4), 459–477,
363 <https://doi.org/10.1007/s00704-013-0854-8>, 2013.
- 364 Denise, C., Rogers, W., & Beringer, J.: Describing rainfall in northern Australia using multiple climate indices, 597–
365 615. <https://doi.org/10.5194/bg-14-597-2017>, 2017.
- 366 Department of Agriculture Sri Lanka.: Climate zones of Sri Lanka., available at:
367 https://www.doa.gov.lk/images/weather_climate/Climatezone.jpg, last access: 7 November 2017
- 368 Department of Meteorology Sri Lanka.: Climate of Sri Lanka., available at:
369 http://www.meteo.gov.lk/index.php?option=com_content&view=article&id=94&Itemid=310&lang=en, last access:
370 7 November 2017
- 371 Dettinger, M. D., & Diaz, H. F.: Global Characteristics of Stream Flow Seasonality and Variability, *Journal of*
372 *Hydrometeorology*, 1(4), 289–310. [https://doi.org/10.1175/1525-7541\(2000\)001<0289:GCOSFS>2.0.CO;2](https://doi.org/10.1175/1525-7541(2000)001<0289:GCOSFS>2.0.CO;2), 2000.
- 373 Easterling, D. R., Meehl, G. A., Parmesan, C., Changnon, S. A., Karl, T. R., & Mearns, L. O.: Climate extremes:
374 Observations, modeling, and impacts. *Science*, 289(5487), 2068–2074.
375 <https://doi.org/10.1126/science.289.5487.2068>, 2000.
- 376 Eden, J. M., Van Oldenborgh, G. J., Hawkins, E., & Suckling, E. B.: A global empirical system for probabilistic
377 seasonal climate prediction. *Geoscientific Model Development*, 8(12), 3947–3973. <https://doi.org/10.5194/gmd-8-3947-2015>, 2015.
- 379 Gerlitz, L., Vorogushyn, S., Apel, H., Gafurov, A., Unger-Shayesteh, K., & Merz, B. A.: Statistically based
380 seasonal precipitation forecast model with automatic predictor selection and its application to central and south Asia.
381 *Hydrology and Earth System Sciences*, 20(11), 4605–4623. <https://doi.org/10.5194/hess-20-4605-2016>, 2016.
- 382 International research institute.: ENSO resources, El-Nino teleconnections & La-Nina teleconnections., available at:
383 <http://iri.columbia.edu/our-expertise/climate/enso/>, 2017a, last access: 1 January 2017.
- 384 International research institute.: IRI ENSO forecast. available at: <http://iri.columbia.edu/our-expertise/climate/forecasts/enso/current>, 2017b, last access: 1 January 2017.
- 386 International Research Institute for Climate Society.: IRI Seasonal Precipitation Forecast., available at:
387 http://iridl.ldeo.columbia.edu/maproom/Global/Forecasts/NMME_Seasonal_Forecasts/Precipitation_ELR.html,
388 2018, last access: 12 February 2018.
- 389 James, G., Witten, D., Hastie, T., & Tibshirani, R.: Springer Texts in Statistics An Introduction to Statistical
390 Learning - with Applications in R. <https://doi.org/10.1007/978-1-4614-7138-7>, 2013.
- 391 Japan Agency for Marine Earth Science and Technology.: SST/DMI data set. available at:

- 392 <http://www.jamstec.go.jp/frcgc/research/d1/iod/DATA/dmi.monthly.txt>, 2017.
- 393 Jentsch, A., Kreyling, J., & Beierkuhnlein, C.: A new generation of events , not trends experiments. *Frontiers in*
394 *Ecology and the Environment*, 5(7), 365–374. [https://doi.org/10.1890/1540-9295\(2007\)5\[365:ANGOCE\]2.0.CO;2](https://doi.org/10.1890/1540-9295(2007)5[365:ANGOCE]2.0.CO;2),
395 2007.
- 396 Jha, S., Sehgal, V. K., Raghava, R., & Sinha, M.: Teleconnections of ENSO and IOD to summer monsoon and rice
397 production potential of India. *Dynamics of Atmospheres and Oceans*, 76, 93–104.
398 <https://doi.org/10.1016/j.dynatmoce.2016.10.001>, 2016.
- 399 Knapp, A. K., Hoover, D. L., Wilcox, K. R., Avolio, M. L., Koerner, S. E., La Pierre, K. J., Smith, M. D.:
400 Characterizing differences in precipitation regimes of extreme wet and dry years: Implications for climate change
401 experiments. *Global Change Biology*, 21(7), 2624–2633. <https://doi.org/10.1111/gcb.12888>, 2015.
- 402 Korecha, D., & Sorteberg, A. Validation of operational seasonal rainfall forecast in Ethiopia. *Water Resources*
403 *Research*, 49(11), 7681–7697. <https://doi.org/10.1002/2013WR013760>, 2013.
- 404 Lee, H.: General Rainfall Patterns in Indonesia and the Potential Impacts of Local Seas on Rainfall Intensity. *Water*,
405 7(4), 1751–1769. <https://doi.org/10.3390/w7041751>, 2015.
- 406 Löwe, R., Madsen, H., & McSharry, P.: Objective classification of rainfall in northern Europe for online operation
407 of urban water systems based on clustering techniques. *Water (Switzerland)*, 8(3).
408 <https://doi.org/10.3390/w8030087>, 2016.
- 409 Maity, R., & Nagesh Kumar, D.: Bayesian dynamic modeling for monthly Indian summer monsoon rainfall using El
410 Niño-Southern Oscillation (ENSO) and Equatorial Indian Ocean Oscillation (EQUINOO). *Journal of Geophysical*
411 *Research Atmospheres*, 111(7), 1–12. <https://doi.org/10.1029/2005JD006539>, 2006.
- 412 Malmgren, B. A., Hullugalla, R., Lindeberg, G., Inoue, Y., Hayashi, Y., & Mikami, T.: Oscillatory behavior of
413 monsoon rainfall over Sri Lanka during the late 19th and 20th centuries and its relationships to SSTs in the Indian
414 Ocean and ENSO. *Theoretical and Applied Climatology*, 89(1–2), 115–125. <https://doi.org/10.1007/s00704-006-0225-9>, 2007.
- 416 Malmgren, B. A., Hulugalla, R., Hayashi, Y., & Mikami, T.: Precipitation trends in Sri Lanka since the 1870s and
417 relationships to El Niño-southern oscillation. *International Journal of Climatology*, 23(10), 1235–1252.
418 <https://doi.org/10.1002/joc.921>, 2003.
- 419 Manchanayake, P., & Madduma Bandara, C.: *Water Resources of Sri Lanka*. Sri Lanka: National Science
420 Foundation, Sri Lanka. Retrieved from http://thakshana.nsf.ac.lk/slstic/NA-202/NA_202.pdf, 1999.
- 421 National Center for Atmospheric Research.: NINO SST Indices (NINO 1+2, 3, 3.4, 4; ONI and TNI). Retrieved
422 from <https://climatedataguide.ucar.edu/climate-data/nino-sst-indices-nino-12-3-34-4-oni-and-tni>, 2018.
- 423 National Oceanic and Atmospheric Administration.: El Nino Southern oscilation., available at:
424 http://www.esrl.noaa.gov/psd/enso/past_events.html, 2017.
- 425 National Oceanic and Atmospheric Administration.: Three Months Outlook, Official Forecast, Climate Prediction
426 Center, National Weather Services., available at:
427 http://www.cpc.ncep.noaa.gov/products/predictions/long_range/seasonal.php?lead=6, last access: 12 February 2018,
- 428 Nur'utami, M. N., & Hidayat, R.: Influences of IOD and ENSO to Indonesian Rainfall Variability: Role of
429 Atmosphere-ocean Interaction in the Indo-pacific Sector. *Procedia Environmental Sciences*, 33, 196–203.
430 <https://doi.org/10.1016/j.proenv.2016.03.070>, 2016.
- 431 Ouyang, R., Liu, W., Fu, G., Liu, C., Hu, L., & Wang, H.: Linkages between ENSO/PDO signals and precipitation,

- 432 streamflow in China during the last 100 years. *Hydrology and Earth System Sciences*, 18(9), 3651–3661.
433 <https://doi.org/10.5194/hess-18-3651-2014>, 2014.
- 434 Power, S., Casey, T., Folland, C., Colman, A., & Mehta, V.: Inter-decadal modulation of the impact of ENSO on
435 Australia. *Climate Dynamics*, 15(5), 319–324. <https://doi.org/10.1007/s003820050284>, 1999.
- 436 Qiu, Y., Cai, W., Guo, X., & Ng, B.: The asymmetric influence of the positive and negative IOD events on China's
437 rainfall. *Scientific Reports*, 4, 4943. <https://doi.org/10.1038/srep04943>, 2014.
- 438 Ranatunge, E., Malmgren, B. A., Hayashi, Y., Mikami, T., Morishima, W., Yokozawa, M., & Nishimori, M.:
439 Changes in the Southwest Monsoon mean daily rainfall intensity in Sri Lanka: Relationship to the El Niño-Southern
440 Oscillation. *Palaeogeography, Palaeoclimatology, Palaeoecology*, 197(1–2), 1–14. [https://doi.org/10.1016/S0031-0182\(03\)00383-3](https://doi.org/10.1016/S0031-0182(03)00383-3), 2003.
- 442 Reason, C. J. C., Landman, W., & Tennant, W.: Seasonal to decadal prediction of southern African climate and its
443 links with variability of the Atlantic ocean. *Bulletin of the American Meteorological Society*, 87(7), 941–955.
444 <https://doi.org/10.1175/BAMS-87-7-941>, 2006.
- 445 Ropelewski C.F. and Halpert M.S.: Quantifying Southern Oscillation-Precipitation Relationships. *Journal of*
446 *Climate.*, 1995.
- 447 Schneider, T., Bischoff, T., & Haug, G. H.: Migrations and dynamics of the intertropical convergence zone. *Nature*,
448 513(7516), 45–53. <https://doi.org/10.1038/nature13636>, 2014.
- 449 Seibert, M., Merz, B., & Apel, H.: Seasonal forecasting of hydrological drought in the Limpopo Basin: A
450 comparison of statistical methods. *Hydrology and Earth System Sciences*, 21(3), 1611–1629.
451 <https://doi.org/10.5194/hess-21-1611-2017>, 2017.
- 452 Singhrattna, N., Rajagopalan, B., Clark, M., & Kumar, K. K.: Seasonal forecasting of Thailand summer monsoon
453 rainfall. *International Journal of Climatology*, 25(5), 649–664. <https://doi.org/10.1002/joc.1144>, 2005.
- 454 Singhrattna, N., Rajagopalan, B., Krishna Kumar, K., & Clark, M.: Interannual and interdecadal variability of
455 Thailand summer monsoon season. *Journal of Climate*, 18(11), 1697–1708. <https://doi.org/10.1175/JCLI3364.1>,
456 2005.
- 457 Smith, M. D.: The ecological role of climate extremes: Current understanding and future prospects. *Journal of*
458 *Ecology*, 99(3), 651–655. <https://doi.org/10.1111/j.1365-2745.2011.01833.x>, 2011.
- 459 Suppiah, R.: Spatial and temporal variations in the relationships between the southern oscillation phenomenon and
460 the rainfall of Sri Lanka, *International Journal of Climatology*, 16(12), 1391–1407.
461 [https://doi.org/10.1002/\(SICI\)1097-0088\(199612\)16:12<1391::AID-JOC94>3.0.CO;2-X](https://doi.org/10.1002/(SICI)1097-0088(199612)16:12<1391::AID-JOC94>3.0.CO;2-X), 1996.
- 462 Surendran, S., Gadgil, S., Francis, P. A., & Rajeevan, M.: Prediction of Indian rainfall during the summer monsoon
463 season on the basis of links with equatorial Pacific and Indian Ocean climate indices. *Environmental Research*
464 *Letters*, 10(9), 094004. <https://doi.org/10.1088/1748-9326/10/9/094004>, 2015.
- 465 Verdon, D. C., & Franks, S. W.: Indian Ocean sea surface temperature variability and winter rainfall: Eastern
466 Australia. *Water Resources Research*, 41(9), 1–10. <https://doi.org/10.1029/2004WR003845>, 2005.
- 467 Ward, P. J., Eisner, S., Flo Rke, M., Dettinger, M. D., & Kummerow, M. Annual flood sensitivities to el nintild;O-
468 Southern Oscillation at the global scale. *Hydrology and Earth System Sciences*, 18(1), 47–66.
469 <https://doi.org/10.5194/hess-18-47-2014>, 2014.
- 470 Whitaker, D. W., Wasimi, S. A., & Islam, S.: The El Niño - Southern Oscillation and Long-Range the Forecastong
471 of Flows in the Ganges, *International Journal of Climatology*, 21(1), 77–87, 2001.

472 Zubair, L.: El Niño-southern oscillation influences on the Mahaweli streamflow in Sri Lanka. International Journal
473 of Climatology, 23(1), 91–102. <https://doi.org/10.1002/joc.865>, 2003.

474 Zubair, L., & Ropelewski, C. F.: The strengthening relationship between ENSO and northeast monsoon rainfall over
475 Sri Lanka and southern India. Journal of Climate, 19(8), 1567–1575. <https://doi.org/10.1175/JCLI3670.1>, 2006.

476

477 **Appendix: Identifying ENSO Influences on Rainfall with Classification** 478 **Models: Implications for Water Resource Management of Sri Lanka**

479 **Normality Testing:**

480 The Shapiro-Wilk’s method is used to identify the normality of rainfall anomaly distribution. The Manampitiya NEM
481 normality test results are given below as an example.

482 Data 1: original data

483 $W = 0.96675$, $p\text{-value} = 0.08185$

484 Data 2: data transformed by square root

485 $W = 0.98772$, $p\text{-value} = 0.7772$

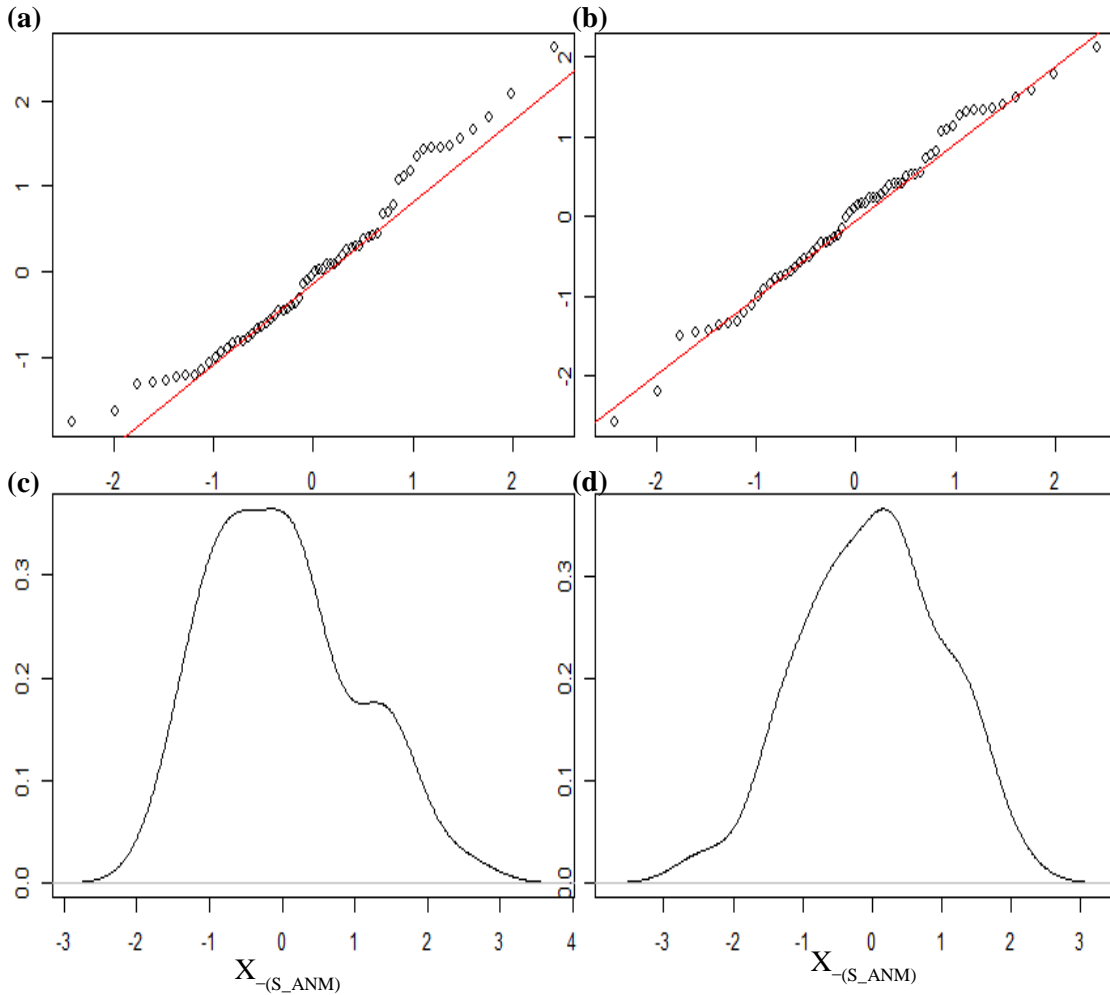
486 Data 3: data transformed by log

487 $W = 0.91577$, $p\text{-value} = 0.0003325$

488 Further, from data plots (Fig. A 1) and the S-W statistic, we conclude that the square root transformed data is closer
489 to being normally distributed than the other forms.

490

491

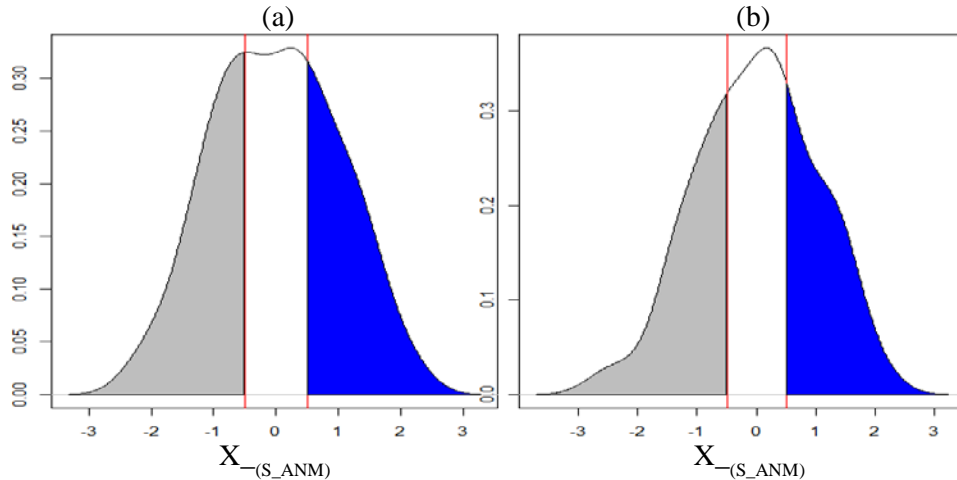


492

493 **Figure A 1** Manampitiya NEM standardized data (a) original form qqplot (b) square root form qqplot (c) original
 494 form density plot (d) square root form density plot

495 **Classification of data**

496 Using 0.5 as a threshold for a normal distribution defines portions of the data that are fairly evenly distributed into
 497 three categories – about 31%, 38%, and 31% for a normal distribution (Fig. A 2). We deemed this a reasonable choice
 498 for our analysis.

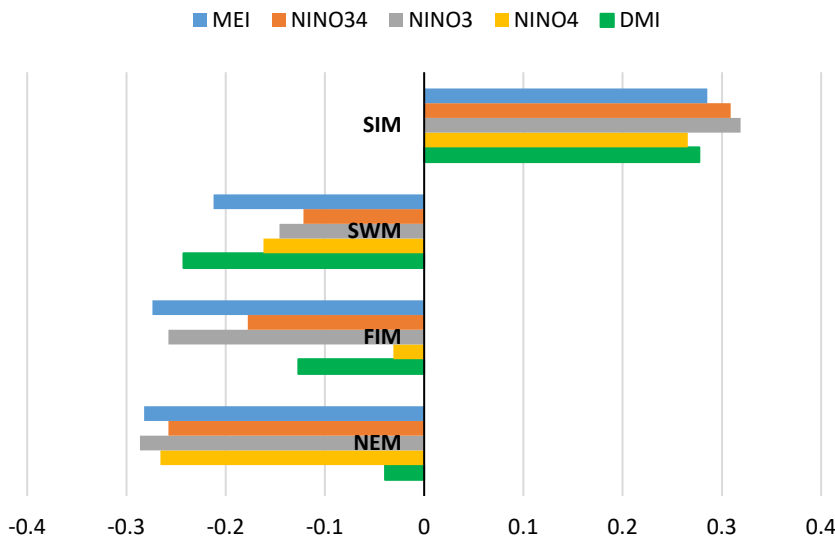


499

500 **Figure A 2** (a) Norton Bridge SWM rainfall anomaly distribution (b) Manampitiya NEM rainfall anomaly distribution

501 **Correlation analysis with multiple climate indices**

502 We examined the correlation between rainfall anomalies and multiple climate indices to choose the two climate indices
 503 MEI and DMI (Fig. A 3, Table A. 1). The ENSO phenomenon is represented by MEI, NINO34, NINO3, NINO4
 504 indices. Correlation analysis indicates that MEI, which is estimated using several climate factors such as sea-level
 505 pressure, zonal and meridional components of the surface wind, sea surface temperature, surface air temperature, and
 506 total cloudiness fraction of the sky (National Oceanic and Atmospheric Administration, 2017), demonstrates higher
 507 correlation with rainfall anomalies in sub-basins for all rainfall seasons compared to the NINO34, NINO3 and NINO4.
 508 The Indian Ocean dipole phenomenon is represented by the DMI index, which represents the gradient of the sea
 509 surface temperature. Based on the correlation analysis and the content of the indices, we selected MEI as the indicator
 510 for ENSO and DMI as the indicator for IOD.



511

512 **Figure A 3** Correlation between Norwood rainfall anomalies with multiple climate indices

513 **Table A. 1** Correlation analysis of rainfall anomalies and climate indices

Rainfall		Morape				Peradeniya				
Month	MEI	NINO34	NINO3	NINO4	DMI	MEI	NINO34	NINO3	NINO4	DMI
NEM	-0.35	-0.35	-0.34	-0.38	-0.09	-0.38	-0.40	-0.39	-0.42	-0.11
FIM	-0.28	-0.19	-0.28	-0.07	-0.11	-0.27	-0.18	-0.30	-0.06	-0.06
SWM	-0.35	-0.24	-0.23	-0.26	-0.29	-0.35	-0.26	-0.25	-0.27	-0.31
SIM	0.21	0.23	0.27	0.19	0.12	0.17	0.19	0.21	0.15	0.09
Rainfall		Laxapana				Norwood				
Month	MEI	NINO34	NINO3	NINO4	DMI	MEI	NINO34	NINO3	NINO4	DMI
NEM	-0.27	-0.26	-0.28	-0.27	-0.01	-0.28	-0.26	-0.29	-0.27	-0.04
FIM	-0.28	-0.16	-0.27	-0.03	-0.07	-0.27	-0.18	-0.26	-0.03	-0.13
SWM	-0.3	-0.23	-0.21	-0.25	-0.31	-0.21	-0.12	-0.15	-0.16	-0.24
SIM	0.1	0.10	0.14	0.06	0.08	0.29	0.31	0.32	0.27	0.28
Rainfall		Randenigala				Bowatenna				
Month	MEI	NINO34	NINO3	NINO4	DMI	MEI	NINO34	NINO3	NINO4	DMI
NEM	-0.30	-0.31	-0.29	-0.34	-0.11	-0.35	-0.36	-0.35	-0.38	-0.2
FIM	-0.29	-0.23	-0.33	-0.10	-0.04	-0.23	-0.17	-0.25	-0.09	-0.02
SWM	-0.17	-0.12	-0.09	-0.18	-0.24	-0.18	-0.09	-0.05	-0.11	-0.12
SIM	0.37	0.38	0.41	0.36	0.35	0.35	0.41	0.40	0.40	0.36
Rainfall		Norton Bridge				Manampitiya				
Month	MEI	NINO34	NINO3	NINO4	DMI	MEI	NINO34	NINO3	NINO4	DMI
NEM	-0.32	-0.30	-0.33	-0.33	-0.01	-0.26	-0.28	-0.26	-0.28	-0.16
FIM	-0.18	-0.12	-0.21	-0.01	-0.08	-0.2	-0.17	-0.31	-0.06	-0.14
SWM	-0.31	-0.22	-0.21	-0.22	-0.37	-0.07	0.08	0.08	-0.01	-0.03
SIM	0.02	-0.02	0.03	-0.04	-0.15	0.45	0.46	0.44	0.46	0.51

514
 515 **Correlation analysis with MEI and DMI climate indices**
 516 Correlation coefficients between rainfall anomalies and MEI and DMI are negative for the NEM, FIM and SWM
 517 seasons and positive for the SIM season. Rainfall anomalies correlations to the DMI are not stronger as the correlations
 518 to the MEI. However, there are strong correlations for the anomalies of major monsoons to the sub basins and DMI
 519 values. For example, wet sub basins (Morape, Peradeniya, Laxapana, Norwood, Norton Bridge) have high correlation
 520 coefficient between SWM rainfall anomalies and DMI, while dry zone (Manampitiya) and intermediate zone
 521 (Randenigala, Bowatenna) sub basins have high correlation coefficient between NEM and SIM rainfall anomalies.

522 **Table A. 2** Correlation between rainfall anomalies and MEI, DMI indices. High correlation coefficients are
 523 highlighted.

Rainfall	Morape		Peradeniya		Randenigala		Bowatenna	
Month	MEI	DMI	MEI	DMI	MEI	DMI	MEI	DMI
NEM	-0.35	-0.09	-0.38	-0.11	-0.30	-0.11	-0.35	-0.20

FIM	-0.28	-0.11	-0.27	-0.06	-0.29	-0.04	-0.23	-0.02
SWM	-0.35	-0.29	-0.35	-0.31	-0.17	-0.24	-0.18	-0.12
SIM	0.21	0.12	0.17	0.09	0.37	0.35	0.35	0.36
Rainfall	Laxapana		Norwood		Norton Bridge		Manampitiya	
Month	MEI	DMI	MEI	DMI	MEI	DMI	MEI	DMI
NEM	-0.27	-0.01	-0.28	-0.04	-0.32	-0.01	-0.26	-0.16
FIM	-0.28	-0.07	-0.27	-0.13	-0.18	-0.08	-0.20	-0.14
SWM	-0.30	-0.31	-0.21	-0.24	-0.31	-0.37	-0.07	-0.03
SIM	0.10	0.08	0.29	0.28	0.02	-0.15	0.45	0.51

524

525 Classification methods classification tree models, random forest and quadratic discriminant analysis identify the
526 relationship between standardized rainfall anomaly classes (dry, average, wet) and MEI and DMI values (Fig. A 4,
527 Fig. A 5, Fig. A 6, Fig. A 7). Positive values of MEI and DMI values resulted dry or average rainfall class for the
528 NEM, FIM and SWM seasons. However, for SIM rainfall has wet or average class for the positive values of MEI and
529 DMI. Accuracy of model result are high for the dominant monsoon rainfall seasons of each sub basin (Table A. 3,
530 Table A. 4, Table A. 5). Ensemble model approach with random forest has given comparatively lower out-of-bag error
531 rate for the dominant monsoons' rainfall anomaly classification (Table A. 5). For example, wet zone sub basins such
532 as Norton Bridge, Norwood, Laxapana, Peradeniya and Morape random forest error rate is lower for the SWM and
533 SIM seasons. Same as, dry and intermediate sub basins Manampitiya, Randenigala and Bowatenna NEM and SIM
534 rainfall classes accuracy rate is high than other rainfall seasons. Also all three models have higher accuracy rate in
535 identifying dry events and error rate of identifying wet and dry class also less 15% (Table A. 3, Table A. 4, Table A.
536 5). Further analysis of two rainfall classes dry and not dry rainfall classes are identified relevant to the MEI and DMI
537 values with classification tree and random forest methods (Fig. A 8, Fig. A 9). Classification tree models for two
538 classes have higher accuracy rate as 65% - 84% for eight sub basins (Table A. 6). Random forest out-of-bag error for
539 two classes models are vary between 20% - 39% and shows higher skill in identifying rainfall classes for major
540 monsoons of the sub basins (Table A. 7). MEI shows higher variable importance of identifying the rainfall classes
541 compare to the DMI values. Specially, for NEM and SIM which are important to the dry zone sub basins importance
542 of MEI is high in the classification. However, some of the wet zone sub basins shows equal importance of DMI
543 variable in identifying two rainfall classes in FIM and SWM (Fig. A 10).

544

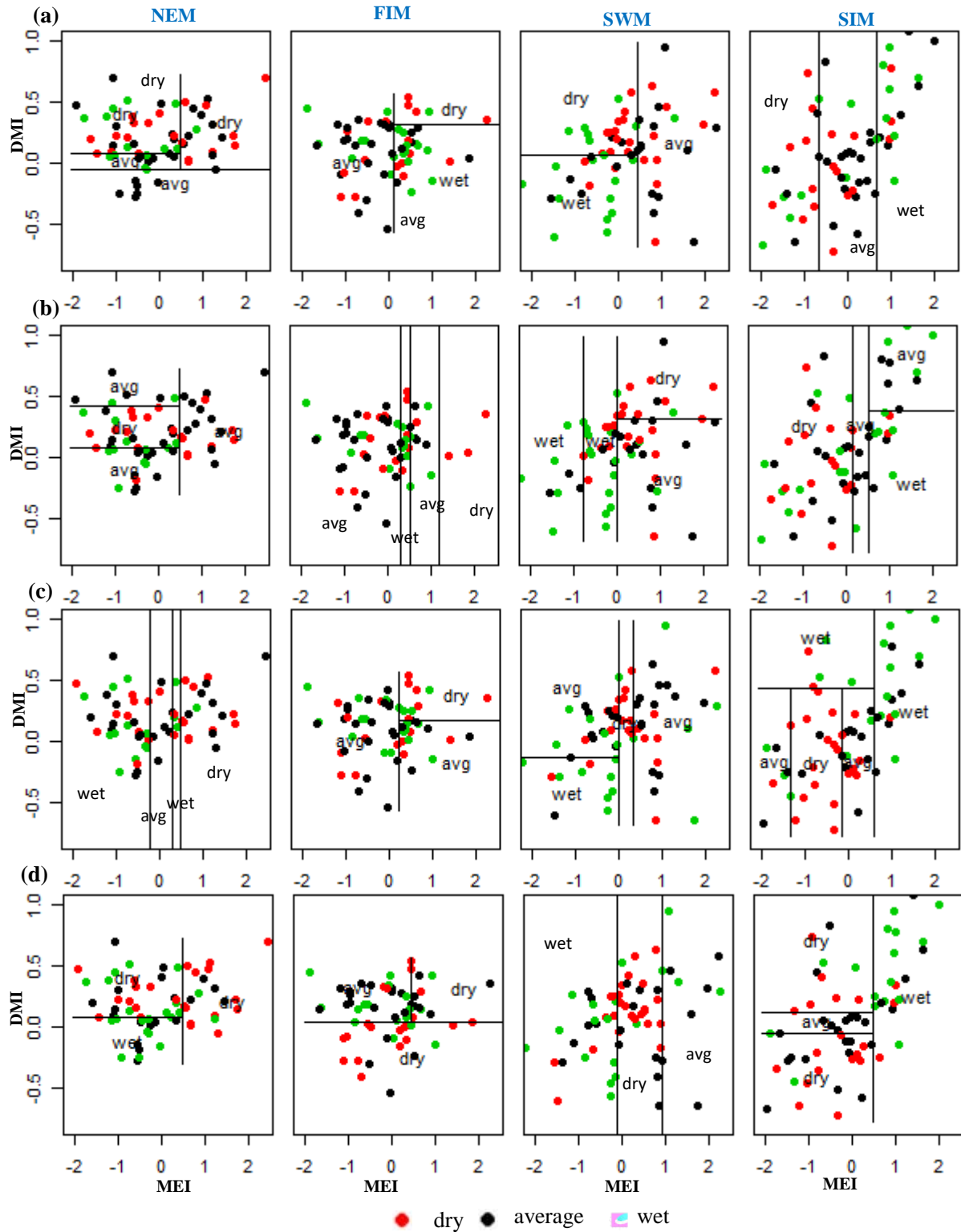
545

546

547

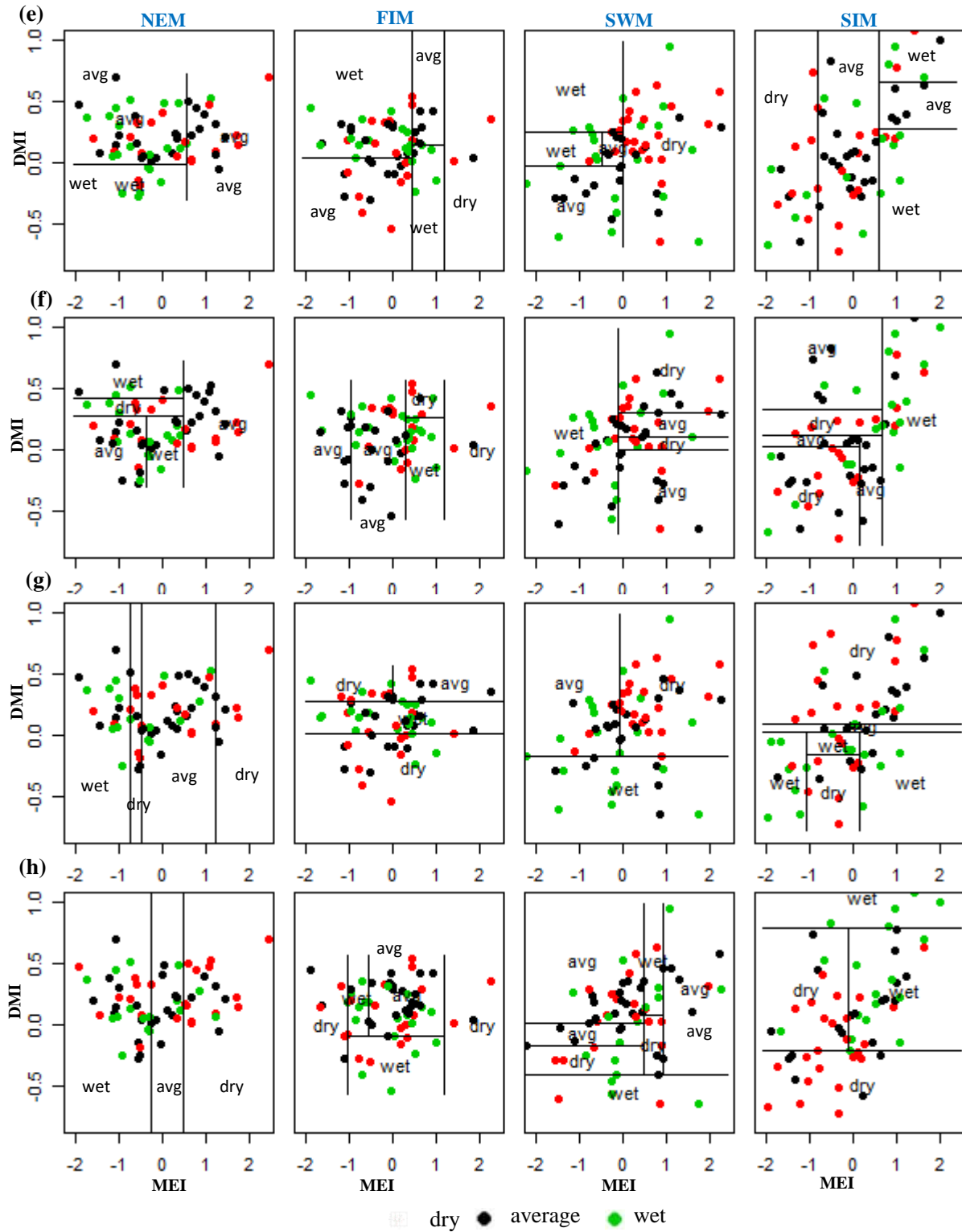
548

549



550

551 **Figure A 4** Identifying relationships between three rainfall classes (dry, average, wet) and MEI and DMI values using classification tree models. (a) Morape (b) Peradeniya (c) Randenigala (d) Bowatenna



552

553 **Figure A 5** Identifying relationships between three rainfall classes (dry, average, wet) and MEI and DMI values
 554 using classification tree models. (e)Laxapana (f)Norwood (g)Norton Bridge (h)Manampitiya

554

555 **Table A. 3** Classification tree model results. Highlighted cells indicate where there may be information content with
 556 respect to forecasting either dry or wet anomaly classes

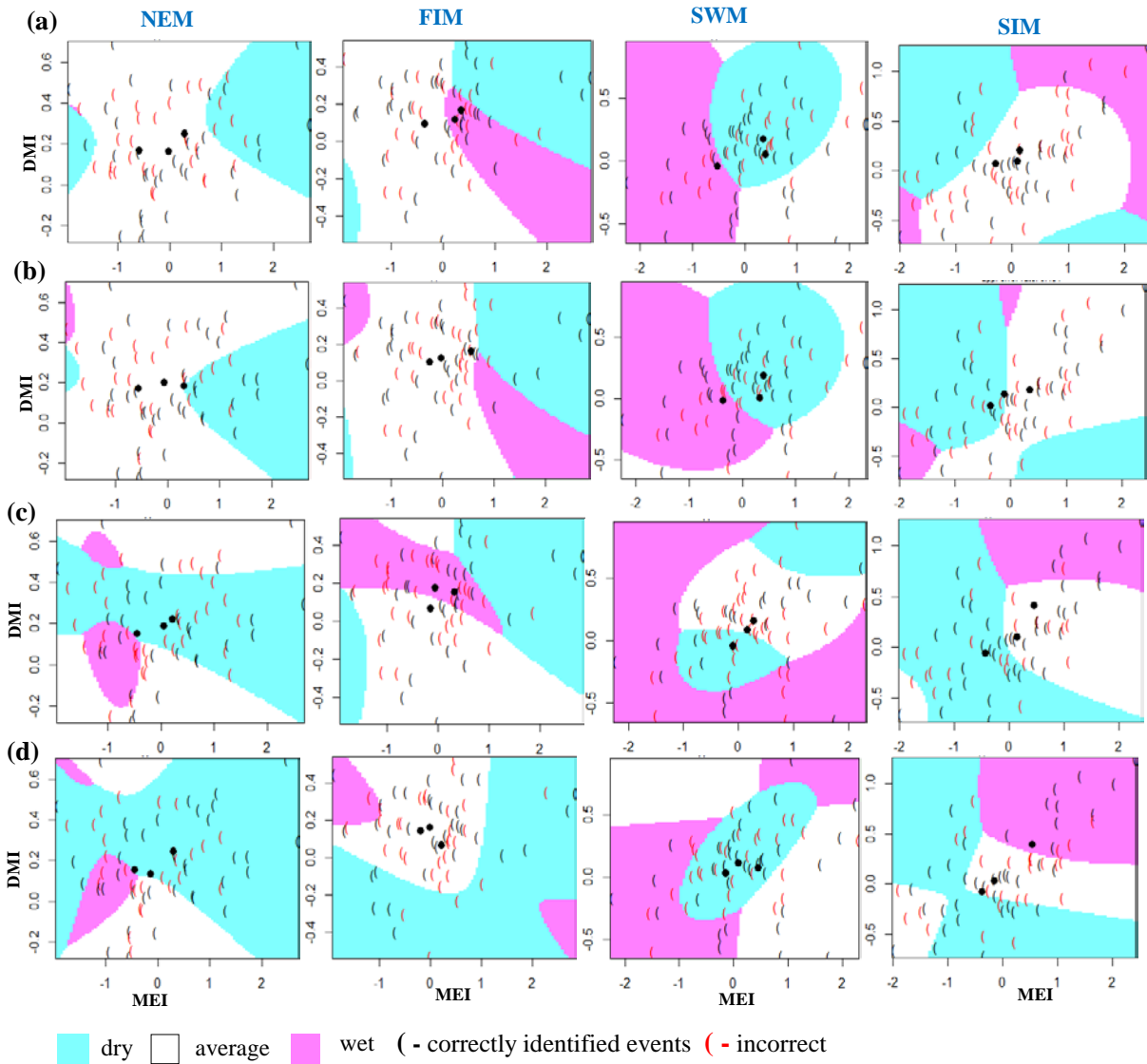
Season	Morape			Peradeniya		
	Dry	Normal	Wet	Dry	Normal	Wet
NEM	21/21	13/29	0/14	10/20	24/31	0/13
FIM	5/19	19/25	12/20	5/20	28/28	6/16
SWM	12/24	13/21	12/19	9/23	11/19	18/22
SIM	8/19	18/28	9/17	12/25	16/19	5/20
Season	Randenigala			Bowatenna		
	Dry	Normal	Wet	Dry	Normal	Wet
NEM	11/24	11/25	12/15	24/24	12/19	0/21
FIM	8/20	24/25	3/19	17/21	17/25	0/18
SWM	8/21	23/24	8/19	18/25	6/21	12/18
SIM	14/24	11/21	15/19	17/21	9/26	13/17
Season	Laxapana			Norwood		
	Dry	Normal	Wet	Dry	Normal	Wet
NEM	0/19	24/24	6/21	4/19	22/28	10/17
FIM	2/20	14/26	18/18	7/19	19/21	12/24
SWM	19/23	14/20	8/21	10/20	14/27	11/17
SIM	8/21	22/26	9/17	16/20	15/25	11/19
Season	Norton Bridge			Manampitiya		
	Dry	Normal	Wet	Dry	Normal	Wet
NEM	11/20	18/29	8/15	12/23	9/25	11/16
FIM	13/21	6/23	15/20	9/21	19/24	8/19
SWM	19/22	8/22	9/20	6/21	25/27	7/16
SIM	19/22	5/22	14/20	20/25	0/20	17/19

557

558

559

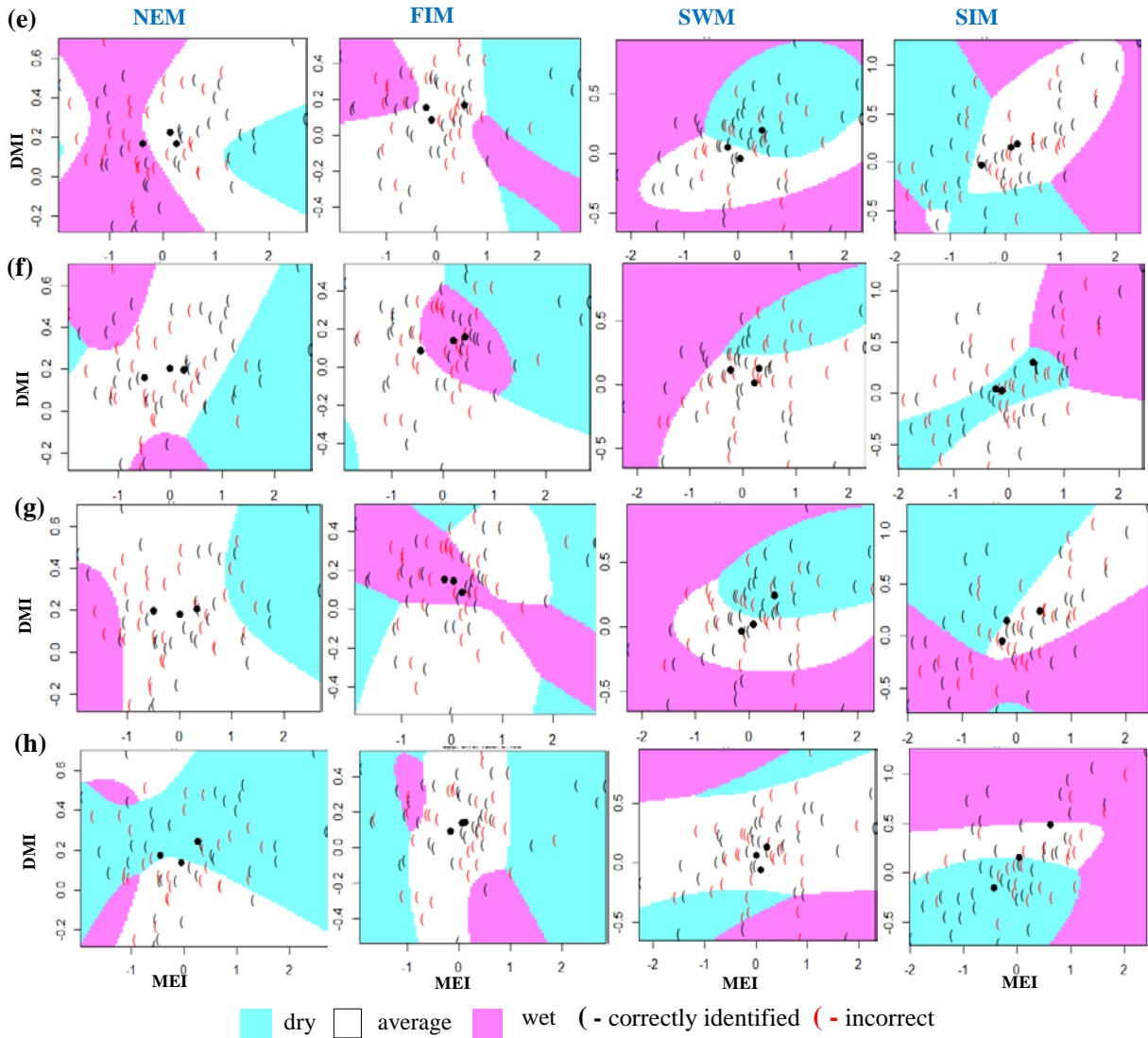
560



561

562

Figure A 6 Identifying relationships between three rainfall classes (dry, average, wet) and MEI and DMI values using QDA models.(a) Morape (b) Peradeniya (c) Randenigala (d) Bowatenna



563

564 **Figure A 7** Identifying relationships between three rainfall classes (dry, average, wet) and MEI and DMI values
 565 using classification tree models. (e) Laxapana (f) Norwood (g) Norton Bridge (h) Manampitiya

566

567

568

569

570

571

572

573

574 **Table A. 4** Classification QDA model results. Highlighted cells indicate where there may be information content
 575 with respect to forecasting either dry or wet anomaly classes

Season	Morape			Peradeniya		
	Dry	Normal	Wet	Dry	Normal	Wet
NEM	6/21	28/29	0/14	10/20	28/31	0/13
FIM	7/19	22/25	9/20	5/20	28/28	2/16
SWM	19/24	6/21	13/19	20/23	6/19	13/22
SIM	5/19	26/28	2/17	13/25	16/19	4/20
Season	Randenigala			Bowatenna		
	Dry	Normal	Wet	Dry	Normal	Wet
NEM	17/24	8/25	4/15	24/24	9/19	3/21
FIM	8/20	13/25	12/19	9/21	23/25	1/18
SWM	4/21	13/24	8/19	19/25	7/21	8/18
SIM	19/24	16/21	6/19	13/21	15/26	10/17
Season	Laxapana			Norwood		
	Dry	Normal	Wet	Dry	Normal	Wet
NEM	4/19	15/24	14/21	8/19	23/28	6/17
FIM	4/20	22/26	8/18	6/19	16/21	13/24
SWM	20/23	13/20	10/21	6/20	19/27	8/17
SIM	9/21	22/26	3/17	11/20	13/25	8/19
Season	Norton Bridge			Manampitiya		
	Dry	Normal	Wet	Dry	Normal	Wet
NEM	5/20	25/29	2/15	22/23	11/25	1/16
FIM	3/20	14/23	14/20	9/21	20/24	5/19
SWM	16/22	9/22	9/20	2/21	26/27	6/16
SIM	7/22	15/22	11/20	17/25	13/20	7/19

576
 577
 578
 579
 580
 581
 582
 583
 584
 585

586 **Table A. 5** Random forest model results. Highlighted cells indicate where there may be information content with
 587 respect to forecasting either dry or wet anomaly classes

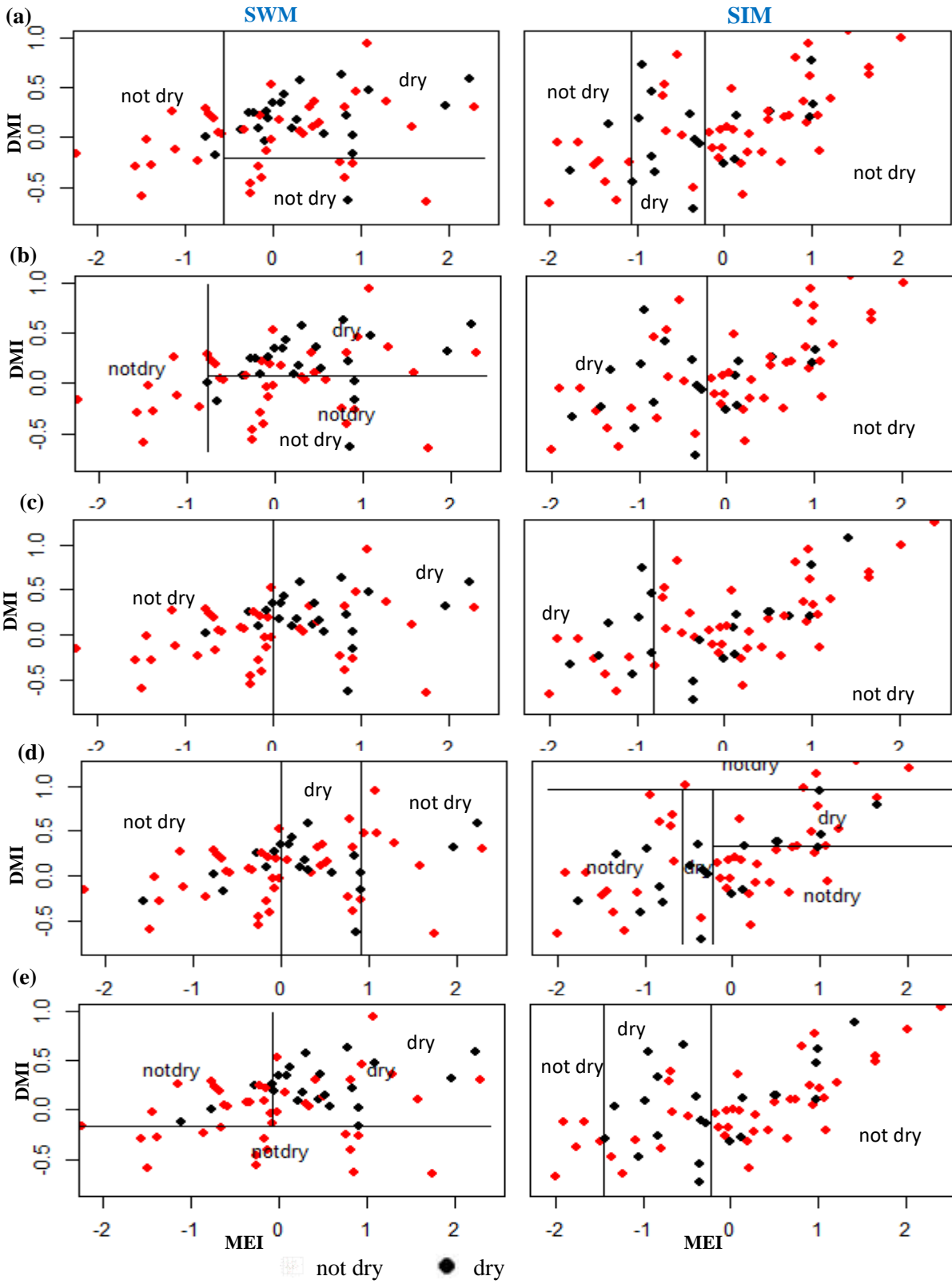
Season	Morape			Peradeniya		
	Dry	Normal	Wet	Dry	Normal	Wet
NEM	12/21	12/29	5/14	9/20	17/31	5/13
FIM	8/19	14/25	10/20	7/20	17/28	6/16
SWM	11/24	6/21	11/19	11/23	1/19	13/22
SIM	8/19	16/28	2/17	5/25	9/19	6/20
Season	Randenigala			Bowatenna		
	Dry	Normal	Wet	Dry	Normal	Wet
NEM	10/24	8/25	4/15	16/24	6/19	11/21
FIM	9/20	8/25	8/19	16/21	14/25	4/18
SWM	9/21	14/24	6/19	14/25	7/21	5/18
SIM	15/24	6/21	7/19	3/21	14/26	11/17
Season	Laxapana			Norwood		
	Dry	Normal	Wet	Dry	Normal	Wet
NEM	3/19	11/24	9/21	9/19	16/28	8/17
FIM	1/20	18/26	1/18	8/19	10/21	12/24
SWM	19/23	9/20	4/21	6/20	15/27	4/17
SIM	10/21	12/26	3/17	8/20	14/25	8/19
Season	Norton Bridge			Manampitiya		
	Dry	Normal	Wet	Dry	Normal	Wet
NEM	11/20	12/29	6/15	14/23	10/25	5/16
FIM	7/21	8/23	8/20	10/21	11/24	6/19
SWM	9/22	6/22	8/20	6/21	17/27	5/16
SIM	13/22	9/22	9/20	15/25	8/20	7/19

588

589

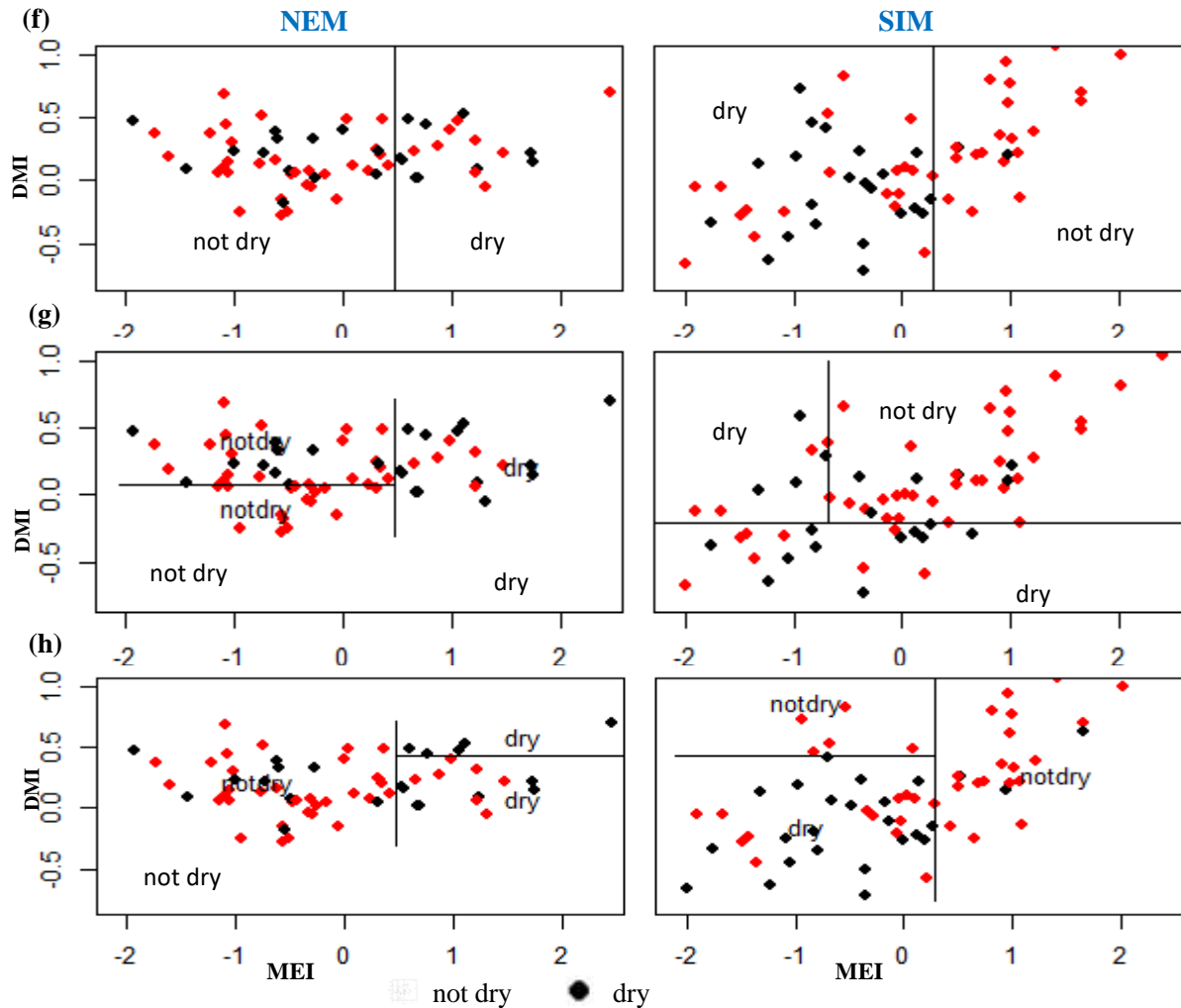
590

591



592

Figure A 8 Identifying relationships between two rainfall classes (dry, not dry) and MEI and DMI values using classification tree models for wet zone sub basins for SWM and SIM seasons. (a) Morape (b) Peradeniya (c) Laxapana (d) Norwood (e) Norton Bridge



593

594 **Figure A 9** Identifying relationships between two rainfall classes (dry, not dry) and MEI and DMI values using
 595 classification tree models for dry and intermediate zone sub basins for NEM and SIM seasons. (f) Randenigala (g)
 596 Bowatenna (h) Manampitiya

597

598 **Table A. 6** Classification tree model results for major rainfall season to the sub basins.

Season	Morape		Peradeniya		Laxapana		Norwood		Norton Bridge	
	Dry	Not dry	Dry	Not dry	Dry	Not dry	Dry	Not dry	Dry	Not dry
SWM	21/24	22/40	18/23	26/41	19/23	27/41	12/20	34/44	19/22	29/42
SIM	10/19	39/45	12/19	30/45	8/21	36/43	11/20	38/44	13/22	36/42
Season	Randenigala		Bowatenna		Manampitiya					
	Dry	Not dry	Dry	Not dry	Dry	Not dry				
NEM	11/24	31/40	14/24	34/40	13/23	34/41				
SIM	23/24	22/40	15/21	32/43	22/25	26/39				

599

600 **Table A. 7** Random forest model results.

Season	Morape			Peradeniya		
	Dry	Not dry	OOB Error	Dry	Not dry	OOB Error
NEM	10/21	33/43	33%	8/20	34/44	34%
FIM	5/19	36/45	36%	6/20	37/44	33%
SWM	11/24	29/40	38%	11/23	28/41	39%
SIM	5/19	39/45	33%	5/19	37/45	34%
Season	Randenigala			Bowatenna		
	Dry	Not dry	OOB Error	Dry	Not dry	OOB Error
NEM	8/24	31/40	39%	15/24	33/40	25%
FIM	6/20	39/44	30%	13/21	38/43	20%
SWM	7/21	38/43	30%	11/25	29/39	38%
SIM	13/24	31/40	31%	6/21	35/43	36%
Season	Laxapana			Norwood		
	Dry	Not dry	OOB Error	Dry	Not dry	OOB Error
NEM	8/20	37/45	30%	10/19	39/45	23%
FIM	7/20	37/44	31%	8/19	39/45	26%
SWM	12/23	27/41	39%	7/20	37/44	31%
SIM	9/21	34/43	33%	7/20	37/44	31%
Season	Norton Bridge			Manampitiya		
	Dry	Not dry	OOB Error	Dry	Not dry	OOB Error
NEM	9/20	36/44	30%	13/23	33/41	28%
FIM	5/21	35/43	38%	8/21	35/43	33%
SWM	9/22	32/42	36%	5/16	34/43	39%
SIM	10/22	36/42	28%	16/25	34/39	22%

601

602

603

604

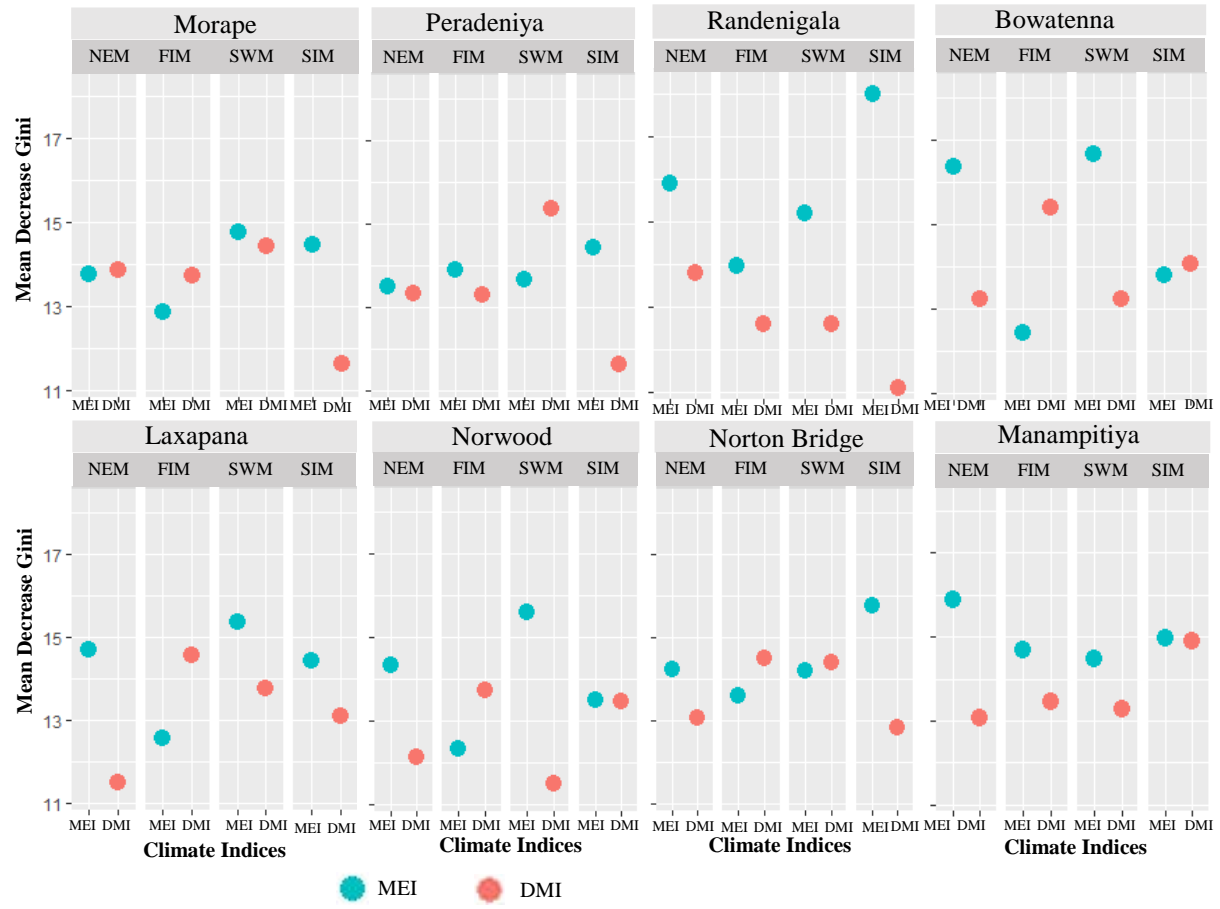
605

606

607

608

609



610

611 **Figure A 10** Random forest importance of variable to identify the dry and not dry classes of rainfall anomalies

612

613

614